Lund TE, Madsen KH, Sidaros K, Luo WL, Nichols TE (2006) Non-white noise in fMRI: does modelling have an impact? Neuroimage 29:54–66.

Lustig C, Snyder AZ, Bhakta M, O'Brien KC, McAvoy M, Raichle ME, Morris JC, Buckner RL (2003) Functional deactivations: change with age and dementia of the Alzheimer type. Proc Natl Acad Sci U S A 100:14504–14509.

Maeshima S, Itakura T, Nakagawa M, Nakai K, Komai N (1997) Visuospatial impairment and activities of daily living in patients with Parkinson's disease: a quantitative assessment of the cube-copying task. Am J Phys Med Rehabil 76:383–388.

Mazoyer B, Zago L, Mellet E, Bricogne S, Etard O, Houdé O, Crivello F, Joliot M, Petit L, Tzourio-Mazoyer N (2001) Cortical networks for working memory and executive functions sustain the conscious resting state in man. Brain Res Bull 54:287–298.

McLean CA, Cherny RA, Fraser FW, Fuller SJ, Smith MJ, Beyreuther K, Bush AI, Masters CL (1999) Soluble pool of Abeta amyloid as a determinant of severity of neurodegeneration in Alzheimer's disease. Ann Neurol 46:860–866.

Mintun MA, Larossa GN, Sheline YI, Dence CS, Lee SY, Mach RH, Klunk WE, Mathis CA, DeKosky ST, Morris JC (2006) [11C]PIB in a nondemented population: potential antecedent marker of Alzheimer disease. Neurology 67:446–452.

Montalto MC, Farrar G, Hehir CT (2007) Fibrillar and oligomeric beta-amyloid as distinct local biomarkers for Alzheimer's disease. Ann N Y Acad Sci 1097:239–258.

Mormino EC, Kluth JT, Madison CM, Rabinovici GD, Baker SL, Miller BL, Koeppe RA, Mathis CA, Weiner MW, Jagust WJ (2009) Episodic memory loss is related to hippocampal-mediated beta-amyloid deposition in elderly subjects. Brain 132:1310–1323.

Morris JC (1993) The Clinical Dementia Rating (CDR): current version and scoring rules. Neurology 43:2412–2414.

Nelissen N, Vandenbulcke M, Fannes K, Verbruggen A, Peeters R, Dupont P, Van Laere K, Bormans G, Vandenberghe R (2007) Abeta amyloid deposition in the language system and how the brain responds. Brain 130:2055–2069.

Oshio R, Tanaka S, Sadato N, Sokabe M, Hanakawa T, Honda M (2010) Differential effect of double-pulse TMS applied to dorsal premotor cortex and precuneus during internal operation of visuospatial information. Neuroimage 49:1108–1115.

Ouchi Y, Yoshikawa E, Okada H, Futatsubashi M, Sekine Y, Iyo M, Sakamoto M (1999) Alterations in binding site density of dopamine transporter in the striatum, orbitofrontal cortex, and amygdala in early Parkinson's disease: compartment analysis for beta-CFT binding with positron emission tomography. Ann Neurol 45:601–610.

Ouchi Y, Okada H, Yoshikawa E, Futatsubashi M, Nobezawa S (2001) Absolute changes in regional cerebral blood flow in association with upright posture in humans: an orthostatic PET study. J Nucl Med 42:707–712.

Ouchi Y, Kanno T, Okada H, Yoshikawa E, Shinke T, Nagasawa S, Minoda K, Doi H (2006) Changes in cerebral blood flow under the prone condition with and without massage. Neurosci Lett 407:131–135.

Ouchi Y, Yoshikawa E, Futatsubashi M, Yagi S, Ueki T, Nakamura K (2009) Altered brain serotonin transporter and associated glucose metabolism in Alzheimer disease. J Nucl Med 50:1260–1266.

Owen AM, McMillan KM, Laird AR, Bullmore E (2005) N-back working memory paradigm: a meta-analysis of normative functional neuroimaging studies. Hum Brain Mapp 25:46–59.

Petrella JR, Prince SE, Wang L, Hellegers C, Doraiswamy PM (2007) Prognostic value of posteromedial cortex deactivation in mild cognitive impairment. PLoS One 2:e1104.

Pike KE, Savage G, Villemagne VL, Ng S, Moss SA, Maruff P, Mathis CA, Klunk WE, Masters CL, Rowe CC (2007) Beta-amyloid imaging and memory in non-demented individuals: evidence for preclinical Alzheimer's disease. Brain 130:2837–2844.

Raichle ME (1998) Behind the scenes of functional brain imaging: a historical and physiological perspective. Proc Natl Acad Sci U S A 95:765–772.

Raichle ME, Snyder AZ (2007) A default mode of brain function: a brief history of an evolving idea. Neuroimage 37:1083–1090; discussion 1097–1099.

Raichle ME, Martin WR, Herscovitch P, Mintun MA, Markham J (1983) Brain blood flow measured with intravenous H2(15)O. II. Implementation and validation. J Nucl Med 24:790–798.

Raj D, Anderson AW, Gore JC (2001) Respiratory effects in human functional magnetic resonance imaging due to bulk susceptibility changes. Phys Med Biol 46:3331–3340.

Reisberg B (1986) Dementia: a systematic approach to identifying reversible causes. Geriatrics 41:30–46.

Rentz DM, Locascio JJ, Becker JA, Moran EK, Eng E, Buckner RL, Sperling RA, Johnson KA (2010) Cognition, reserve, and amyloid deposition in normal aging. Ann Neurol 67:353–364.

Rowe CC, Ng S, Ackermann U, Gong SJ, Pike K, Savage G, Cowie TF, Dickinson KL, Maruff P, Darby D, Smith C, Woodward M, Merory J, Tochon-Danguy H, O'Keefe G, Klunk WE, Mathis CA, Price JC, Masters CL, Villemagne VL (2007) Imaging beta-amyloid burden in aging and dementia. Neurology 68:1718–1725.

Sheline YI, Raichle ME, Snyder AZ, Morris JC, Head D, Wang S, Mintun MA (2010) Amyloid plaques disrupt resting state default mode network connectivity in cognitively normal elderly. Biol Psychiatry 67:584–587.

Silverman DH, Small GW, Chang CY, Lu CS, Kung De Aburto MA, Chen W, Czernin J, Rapoport SI, Pietrini P, Alexander GE, Schapiro MB, Jagust WJ, Hoffman JM, Welsh-Bohmer KA, Alavi A, Clark CM, Salmon E, de Leon MJ, Mielke R, Cummings JL, et al. (2001) Positron emission tomography in evaluation of dementia: regional brain metabolism and long-term outcome. JAMA 286:2120–2127.

Simpson JR Jr, Snyder AZ, Gusnard DA, Raichle ME (2001a) Emotion-induced changes in human medial prefrontal cortex: I. During cognitive task performance. Proc Natl Acad Sci U S A 98:683–687.

Simpson JR Jr, Drevets WC, Snyder AZ, Gusnard DA, Raichle ME (2001b) Emotion-induced changes in human medial prefrontal cortex: II. During anticipatory anxiety. Proc Natl Acad Sci U S A 98:688–693.

Sperling RA, Laviolette PS, O'Keefe K, O'Brien J, Rentz DM, Pihlajamaki M, Marshall G, Hyman BT, Selkoe DJ, Hedden T, Buckner RL, Becker JA, Johnson KA (2009) Amyloid deposition is associated with impaired default network function in older persons without dementia. Neuron 63:178–188.

Supekar K, Menon V, Rubin D, Musen M, Greicius MD (2008) Network analysis of intrinsic functional brain connectivity in Alzheimer's disease. PLoS Comput Biol 4:e1000100.

Tzourio-Mazoyer N, Landeau B, Papathanassiou D, Crivello F, Etard O, Delcroix N, Mazoyer B, Joliot M (2002) Automated anatomical labeling of activations in SPM using a macroscopic anatomical parcellation of the MNI MRI single-subject brain. Neuroimage 15:273–289.

Vlassenko AG, Vaishnavi SN, Couture L, Sacco D, Shannon BJ, Mach RH, Morris JC, Raichle ME, Mintun MA (2010) Spatial correlation between brain aerobic glycolysis and amyloid-beta (Abeta) deposition. Proc Natl Acad Sci U S A 107:17763–17767.

Vogt BA, Finch DM, Olson CR (1992) Functional heterogeneity in cingulate cortex: the anterior executive and posterior evaluative regions. Cereb Cortex 2:435–443.

Yanase D, Matsunari I, Yajima K, Chen W, Fujikawa A, Nishimura S, Matsuda H, Yamada M (2005) Brain FDG PET study of normal aging in Japanese: effect of atrophy correction. Eur J Nucl Med Mol Imaging 32:794–805.

Yokokura M, Mori N, Yagi S, Yoshikawa E, Kikuchi M, Yoshihara Y, Wakuda T, Sugihara G, Takebayashi K, Suda S, Iwata Y, Ueki T, Tsuchiya KJ, Suzuki K, Nakamura K, Ouchi Y (2011) In vivo changes in microglial activation and amyloid deposits in brain regions with hypometabolism in Alzheimer's disease. Eur J Nucl Med Mol Imaging 38:343–351.

Zhang HY, Wang SJ, Xing J, Liu B, Ma ZL, Yang M, Zhang ZJ, Teng GJ (2009) Detection of PCC functional connectivity characteristics in resting-state fMRI in mild Alzheimer's disease. Behav Brain Res 197:103–108.

Brain and Behavior

Open Access

Pilot data on telmisartan short-term effects on glucose metabolism in the olfactory tract in Alzheimer's disease

Etsuko Imabayashi[1], Hiroshi Matsuda[1], Kimiko Yoshimaru[2], Ichiei Kuji[1], Akira Seto[3], Yasumasa Shimano[1], Kimiteru Ito[1], Daisuke Kikuta[1], Tomokazu Shimazu[2] & Nobuo Araki[2]

[1]Department of Nuclear Medicine, Saitama Medical University International Medical Center, 1397-1 Yamane, Hidaka, Saitama, Japan
[2]Department of Neurology, Saitama Medial University Hospital, 38 Morohongo, Moroyama, Iruma-gun, Saitama, Japan
[3]Department of Nuclear Medicine, Saitama Medial University Hospital, 38 Morohongo, Moroyama, Iruma-gun, Saitama, Japan

Keywords
Alzheimer's disease (AD), angiotensin II receptor blocker (ARB), telmisartan, ^{18}F-fluorodeoxyglucose positron emission tomography (FDG-PET), anterior olfactory nucleus.

Correspondence
Etsuko Imabayashi M.D., Ph.D., Department of Nuclear Medicine, Saitama Medical University International Medical Center, 1397-1, Yamane, Hidaka, Saitama, 350-1298, Japan. Tel: +81-42-984-4147; Fax: 81-42-984-4146; E-mail: embysh@saitama-med.ac.jp.

Received: 19 April 2011; Revised: 26 July 2011; Accepted: 27 July 2011

doi: 10.1002/brb3.13

Abstract

The possible effect of antihypertensive therapy on Alzheimer's disease (AD) has been studied, and angiotensin II receptor blockers (ARBs) have been suggested to exert an effect on cognitive decline. The purpose of this study is to clarify the functional effects of telmisartan, a long-acting ARB, on AD brain using prospective longitudinal ^{18}F-fluorodeoxyglucose positron emission tomography (FDG-PET) studies. For this purpose, brain glucose metabolism of four hypertensive patients with AD was examined with FDG-PET before and after administration of telmisartan. Studied subjects underwent three FDG-PET studies at intervals of 12 weeks. Antihypertensive treatment except for telmisartan was started after the first FDG-PET and continued for 24 weeks. Then 40–80 mg of telmisartan was added after the second FDG-PET and continued for 12 weeks.Glucose metabolism was significantly decreased during the first 12 weeks without telmisartan use at an area (−10, 21, −22, x, y, z; Z = 3.56) caudal to the left rectal gyrus and the olfactory sulcus corresponding to the left olfactory tract. In contrast, the introduction of telmisartan during the following 12 weeks preserved glucose metabolism at areas (5, 19, −20, x, y, z; Z = 3.09; 6, 19, −22, x, y, z; Z = 2.88) caudal to the bilateral rectal gyri and olfactory sulci corresponding to the bilateral olfactory tracts. No areas showed decreased glucose metabolism after the introduction of telmisartan. In AD, amyloid-β deposition is observed in the anterior olfactory nucleus (AON) of the olfactory tract. Glucose metabolism in AON may be progressively decreased and preserved by telmisartan.

Introduction

Many risk factors for dementia have been epidemiologically investigated with the hope of preventing or delaying the onset of Alzheimer's disease (AD; Korczyn and Vakhapova 2007). Hypertension is linked to AD along with smoking, diabetes mellitus, and hypercholesterolemia (Papademetriou 2005; Kehoe and Wilcock 2007). The possible effect of antihypertensive therapy on AD has been studied, and it is suggested that angiotensin-converting enzyme (ACE) inhibitors and angiotensin II receptor blockers (ARBs) exert a greater effect on cognitive decline than other antihypertensive medications (Gard 2002, 2004).

Telmisartan is a long-acting ARB that is effective for early hypertension. It has in addition peroxisome proliferator-activated receptor gamma (PPARγ) agonist effects (Benson et al. 2004; Lacourcire et al. 2004). Henka et al. (2005) reported that treatment with the PPARγ agonist pioglitazone reduces soluble amyloid-β (Aβ)1–42 peptide in mice. It has been shown that mRNA and protein levels of β-secretase or β-site amyloid precursor protein cleaving enzyme is repressed by pioglitazone resulting in reduction of Aβ1–42 (Sastre et al. 2006). Clinically, PPARγ agonists have been reported to act as insulin sensitizers, and to improve cognition and memory in AD patients (Watson et al. 2005; Landreth 2007). Mogi et al (2008) showed that telmisartan prevented cognitive decline partly due to PPARγ activation. Recently PPARγ activation in the brain has been highlighted to prevent AD via enhancement of Aβ clearance (Camacho et al. 2004) and antiinflammatory effects in neurons (Luna–Medina et al.

© 2011 The Authors. Published by Wiley Periodicals, Inc. This is an open access article under the terms of the Creative Commons Attribution Non-Commercial License, which permits use, distribution and reproduction in any medium, provided the original work is properly cited and is not used for commercial purposes.

2005), endothelial cells (Wang et al. 2002), astrocytes and microglia (Klotz et al. 2003), and an increase in neural stem cell proliferation (Wada et al. 2006; Morales–Garcia et al. 2010). From these findings, it is hoped that treatment of blood pressure (BP) with telmisartan may mitigate the cognitive decline in AD. The purpose of the present study is to clarify the functional effects of telmisartan on AD brain using prospective longitudinal ^{18}F-fluorodeoxyglucose positron emission tomography (FDG-PET) studies. In the revised NINCDS-ADRDA criteria, FDG-PET is dealt with as a topographical marker and is described to be more useful than pathological markers when the first cognitive symptoms are manifest in preclinical AD patients (Dubois et al. 2010).

Materials and Methods

Subjects

Among hypertensive outpatients with memory impairment with systolic blood pressure (SBP) of ≥140 mmHg or diastolic blood pressure (DBP) of 90 mmHg in the Department of Neurology of Saitama Medical University Hospital, those who were clinically diagnosed with AD according to revised NINCDS-ADRDA criteria, were recruited (Dubois et al. 2010). Patients who met the following criteria were excluded: (1) history of allergy to ARB; (2) SBP of ≥160 mmHg or DBP of ≥100 mmHg; (3) pregnancy; (4) severe biliary excretion dysfunction with serum total bilirubin concentration above 2.0 mg/dL; (5) severe liver dysfunction with serum asparatate aminotransferase (AST) or alanine aminotransferase (ALT) above 100IU/L; (6) severe renal dysfunction with serum Cr level above 3.0 mg/dL; (7) hyperkalemia; (8) continuous administration of ARB, ACE inhibitor, or pioglitazone; (9) other conditions deemed inappropriate for the purposes of this study by the investigators. Seven patients who met these criteria were enrolled. FDG-PET findings of all patients were supportive of AD. Of these seven patients, one experienced digestive tract hemorrhage during the follow-up studies and two refused to continue to participate. Finally four AD patients, two men and two women, aged from 70 to 77 years, finished the present longitudinal study protocol. At each FDG-PET study, mini-mental state examination (MMSE) was administered and BP was measured.

This study was approved by the institutional review board of Saitama Medical University International Medical Center and Saitama Medical University Hospital, and all subjects gave written informed consent to participate.

Study protocol

The subjects underwent three FDG-PET studies at intervals of 12 weeks. Antihypertensive treatment except for telmisartan was started immediately after the first FDG-PET study and continued for 24 weeks. Then 40–80 mg of telmisartan was added immediately after the second FDG-PET study and continued for 12 weeks (Fig. 1).

FDG-PET

FDG-PET was performed in the Department of Nuclear Medicine of Saitama Medical University International Medical Center. Before FDG-PET was performed, all subjects had an intravenous line established. Each subject received an intravenous injection of 185 MBq of FDG while lying in the supine position with eyes closed in a dimly lit, quiet room and was kept in the same resting state for at least 20 minutes. Fifty minutes after the injection of FDG, brain PET was performed using PET/Computed Tomography (CT) equipment with high spatial resolution (Biograph 6 Hi-Rez; Siemens Medical Systems, Inc.:Suite, Washington, D.C., United States). The combination of Fourier rebinning and the ordered subsets expectation-maximization at iteration number 4 and subset 16, and Gaussian filter at 6-mm full width at half maximum (FWHM) was used for PET image reconstruction. Attenuation correction was performed using CT data.

Image preprocessing

All FDG-PET images were spatially normalized using statistical parametric mapping 2 (SPM2; http://www.fil.ion.ucl.ac.uk/spm/) to a standardized stereotactic space based on the Talairach and Tournoux (1988) atlas, using 12-parameter linear affine normalization and a further 16 nonlinear iteration algorithms with an original template of FDG (Sakai et al. 2006). Then, isotropic Gaussian smoothing with 12-mm full-width at half maximum was performed.

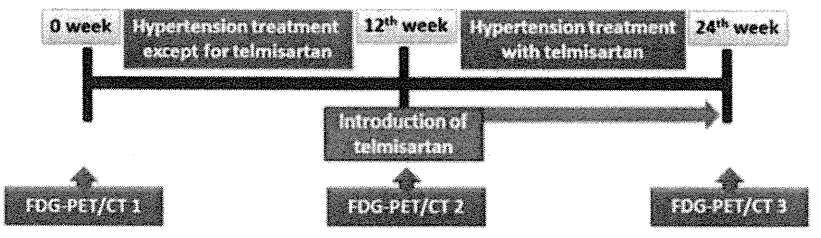

Figure 1. Study protocol. Subjects underwent FDG-PET at three points: the first at entry into this study, the second and third at 12 and 24 weeks after the 1st study, respectively. Telmisartan therapy was started immediately after the second study.

© 2011 The Authors. Published by Wiley Periodicals, Inc.

Image analysis

Data were analyzed also using SPM2 program. The SPM2 combines the general linear model and the theory of Gaussian fields to make statistical inferences about regional effects (Friston et al. 1991, 1994). To examine changes in brain glucose metabolism during the 12 weeks without telmisartan, regionally specific differences between the first and second FDG-PET were statistically assessed using a two-tailed paired contrast testing for a decreased probability of glucose metabolism. Then to examine regionally specific differences in glucose metabolism between the two conditions, with and without telmisartan, the first, second, and third FDG-PET were statistically assessed. A two-tailed contrast testing was used for an increased or decreased probability (multiple subjects with different conditions in SPM2). To exclude time effect in voxel intensity across three scans, the term days was included as a nuisance covariate. The analysis was performed with normalization of global glucose metabolism for each subject to the same mean value with proportional scaling to compare two conditions regarding relative FDG distribution. The gray matter threshold was set to 0.8.

The resulting set of values for each contrast constituted a statistical parametric map of the t statistic SPM {t}. The SPM {t} maps were then transformed to the units of normal distribution (SPM {Z}), and height threshold was set to $P = 0.005$ uncorrected for multiple comparisons with extent threshold to 100 voxels. These areas of significance were visualized as overlaid on a normalized MR image to obtain a clear view of the location of the glucose metabolism changes.

Results

MMSE scores and BP are listed in Table 1. No significant changes in MMSE scores were observed during the time course. SBP declined significantly from the first to third and from the second to third FDG-PET. DBP declined significantly from the first to third FDG-PET.

Glucose metabolism was significantly decreased during the first 12 weeks without telmisartan at an area (−10, 21, −22, x, y, z; $Z = 3.56$) caudal to the left rectal gyrus and the olfactory sulcus corresponding to the left olfactory tract (Fig. 2).

In contrast, the introduction of telmisartan during the following 12 weeks preserved glucose metabolism at areas (5, 19, −20, x, y, z; $Z = 3.09$; −6, 19, −22, x, y, z; $Z = 2.88$) caudal to the bilateral rectal gyri and olfactory sulci corresponding to the bilateral olfactory tracts (Fig. 3). No areas showed decreased glucose metabolism after the introduction of telmisartan.

Discussion

This short-term study showed a significant decline and preservation of glucose metabolism in a localized area caudal to the rectal gyrus corresponding to the olfactory tract during the first 12 weeks without telmisartan, and during the following 12 weeks with telmisartan, respectively.

The localized area corresponding to the olfactory tract detected by statistical analysis of longitudinal FDG-PET studies contains the anterior olfactory nucleus (AON; Saiz–Sanchez et al. 2010). AON plays a central role in human olfactory processing (Price 2004; Brunjes and Kenerson 2010). Though central olfactory connections are scarcely known in man, AON is assumed to have connections to the piriform cortex, anterior amygdala, periamygdaloid cortex, and the rostal entorhinal cortex (Price 2004). In Parkinson's disease, Lerner and Bagic (2008) proposed that AON is connected to the dorsal motor nucleus of the vagus by three principal pathways: the stria medullaris thalami and habenular nuclei, the

Table 1. Subjects' background, blood pressure, and cognitive state.

			Blood pressure						MMSE		
			Systolic			Diastolic			(Score)		
	Age	Gender	First	Second	Third	First	Second	Third	First	Second	Third
Case 1	76	Male	151	148	138	75	78	68	22	25	20
Case 2	77	Male	149	138	130	78	74	70	26	26	25
Case 3	70	Female	159	158	141	90	80	67	21	16	21
Case 4	73	Female	148	145	138	80	50	60	21	21	24

*$P < 0.005$; **$P < 0.01$; §$P < 0.05$.

© 2011 The Authors. Published by Wiley Periodicals, Inc.

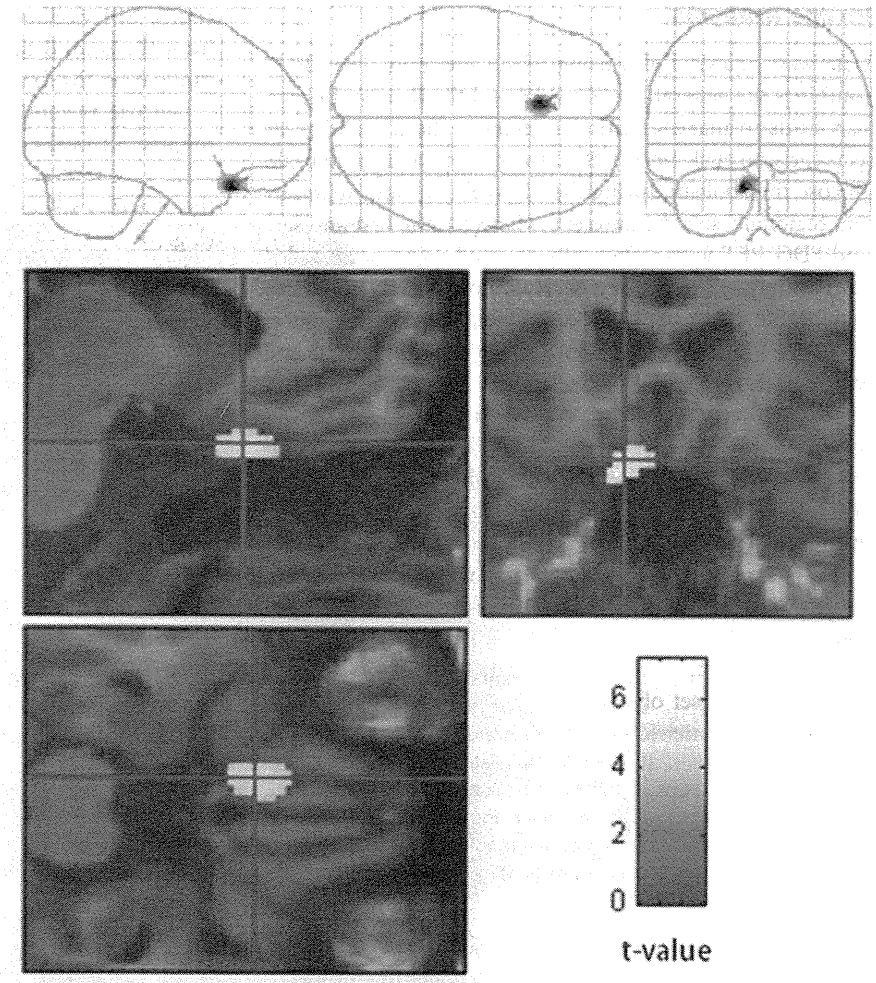

Figure 2. Statistically significant decrease of glucose metabolism from the first to second FDG-PET studies in an area caudal to the left rectal gyrus and the olfactory sulcus corresponding to the left olfactory tract ($P < 0.005$). The SPM of the *t*-statistics is displayed in a standard format as a maximum intensity projection viewed from right-hand side and from the top and the back (top), and as orthogonal sections (bottom).

amygdala and stria terminalis, and the medial forebrain bundle and hypothalamus. Because of these many pathways, AON is assumed to be rich in dendrites and astrocytes, resulting in abundant glucose consumption in this small region (Iadecola and Nedergaard 2007).

Hyposmia has been suggested to be a diagnostic symptom in early AD (Djordjevic et al. 2008). Li et al. (2010) proposed an objective way to reveal olfactory functional deficits in AD patients using a functional MRI. Olfactory functional impairment may result from early neurodegeneration of olfactory systems including AON (Pearson et al. 1985; Braak and Braak 1991; Price et al. 1991). Kovacs et al. (1999) showed that Aβ deposition and neurofibrillary tangle formation are observed in the olfactory bulb both in aging and AD though more frequently in the latter. Moreover, Saiz-Sanchez et al. (2010) analyzed the AON expression levels of somatostatin in AD versus controls, and found that levels of somatostatin were reduced in AON of AD cases compared to controls. It also has been reported that the reduction in somatostatin induces downregulation of neprylisin, a peptidase that catalyzes the proteolytic degradation of Aβ, and that may be a trigger for Aβ accumulation leading to late-onset sporadic AD (Saito et al. 2005). Decreased somatostatin expression may therefore result in Aβ accumulation. Furthermore, a reduction in the density of axons was observed in the olfactory tract of AD patients (Armstrong et al. 2008). Considering such involvement of the olfactory system in AD (Brunjes and Kenerson 2010), glucose metabolism in AON may be decreased more progressively within a short interval than in any other brain region.

Telmisartan is known to effectively reduce Aβ deposition (Mogi et al. 2008) and to induce PPARγ activation. This PPARγ activation has been reported to prevent brain damage through an antiinflammatory effect, for example in endothelial cells, astrocytes, and microglia (Wang et al. 2002; Klotz et al. 2003; Camacho et al. 2004; Heneka et al. 2005; Luna–Medina et al. 2005; Watson et al. 2005; Sastre et al. 2006; Wada et al. 2006; Landreth 2007; Mogi et al. 2008; Morales–Garcia et al. 2010). Thus, the current study supports the contention that progressive AD pathology in AON may be prevented by telmisartan.

© 2011 The Authors. Published by Wiley Periodicals, Inc.

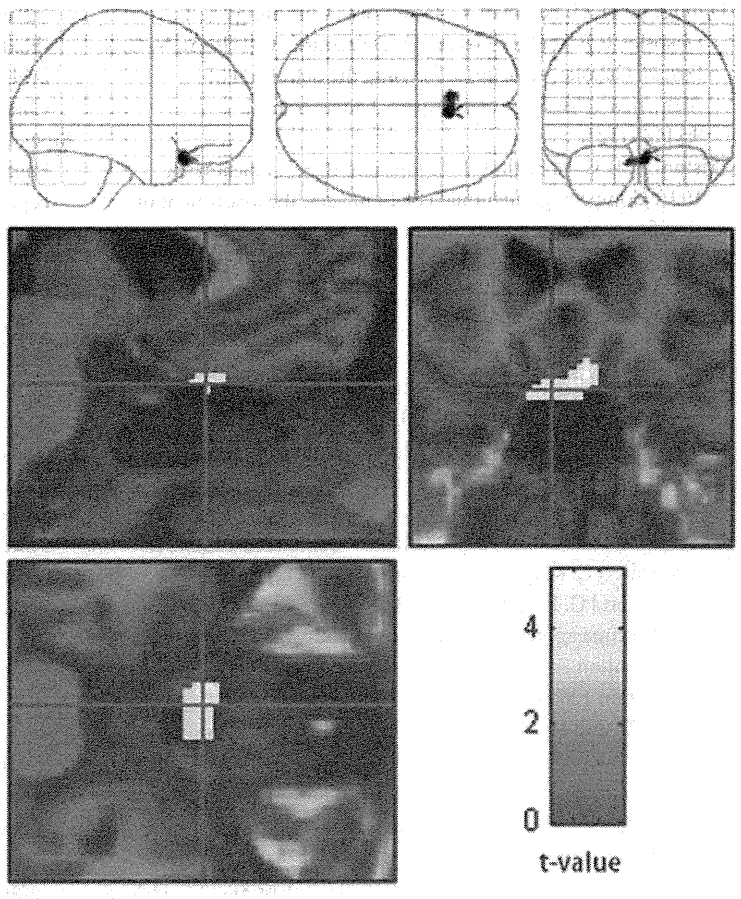

Figure 3. Statistically significant preservation of glucose metabolism by telmisartan from the first and second to third FDG-PET studies in areas caudal to the bilateral rectal gyri and the olfactory sulci corresponding to bilateral olfactory tracts ($P < 0.005$). The SPM of the *t*-statistics is displayed in a standard format as a maximum intensity projection viewed from right-hand side and from the top and the back (top) and as orthogonal sections (bottom).

The present study period may be too short to detect cognitive changes. However, this short term may not be inappropriate to observe any early effect of telmisartan on brain glucose metabolism. Although a further study may be necessary in a larger number of subjects, the current well-localized results with statistical significance may help to define the effect of telmisartan on AD brain.

Conclusion

In consideration of the recent many studies on the olfactory systems in AD, high-resolution FDG-PET is quite useful for the functional evaluation of a small area involving AON. Telmisartan therapy may inhibit short-term decline of glucose metabolism in the olfactory tract in AD brain.

Acknowledgments

We are thankful to the radiology technicians of the Department of Nuclear Medicine of Saitama Medical University International Medical Center for their technical support and to Prof. John Gelblum for proofreading this manuscript.

References

Armstrong, R. A., A. B. Syed, and C. U. Smith. 2008. Density and cross-sectional areas of axons in the olfactory tract in control subjects and Alzheimer's disease: an image analysis study. Neurol. Sci. 29:23–27.

Benson, S. C., H. A. Pershadsingh, C. I. Ho, A. Chittiboyina, P. Desai, M. Pravenec, N. Qi, J. Wang, M. A. Avery, and T. W. Kurtz. 2004. Identification of telmisartan as a unique angiotensin II receptor antagonist with selective PPARgamma-modulating activity. Hypertension 43:993–1002.

Braak, H., and E. Braak. 1991. Neuropathological staging of Alzheimer-related changes. Acta Neuropathol. 82:239–259.

Brunjes P. C., and M. C. Kenerson. 2010. The anterior olfactory nucleus: quantitative study of dendritic morphology. J. Comp. Neurol. 1:1603–1616.

Camacho I. E., L. Serneels, K. Spittaels, P. Merchiers, D. Dominguez, and B. De Strooper. 2004. Peroxisome-proliferator-activated receptor gamma induces a clearance mechanism for the amyloid-beta peptide. J. Neurosci. 1:10908–10917

Djordjevic, J., M. Jones-Gotman, K. De Sousa, and H. Chertkow. 2008. Olfaction in patients with mild cognitive impairment and Alzheimer's disease. Neurobiol. Aging 29:693–706.

© 2011 The Authors. Published by Wiley Periodicals, Inc.

Dubois, B., H. H. Feldman, C. Jacova, J. L. Cummings, S. T. Dekosky, P. Barberger-Gateau, A. Delacourte, G. Frisoni, N. C. Fox, D. Galasko, et al. 2010. Revising the definition of Alzheimer's disease: a new lexicon. Lancet Neurol. 9:1118–1127.

Friston, K. J., C. D. Frith, P. F. Liddle, and R. S. J. Frackowiak. 1991. Comparing functional (PET) images: the assessment of significant change. Cereb. Blood Flow Metab. 11:690–699.

Friston, K. J., K. J. Worsley, R. S. J. Frackowiak, J. C. Mazziotta, and A. C. Evans. 1993. Assessing the significance of focal activations using their spatial extent. Hum. Brain Mapping 1:210 –220.

Gard, P. R. 2002. The role of angiotensin II in cognition and behaviour. Eur. J. Pharmacol. 1:1–14.

Gard, P. R. 2004. Angiotensin as a target for the treatment of Alzheimer's disease, anxiety and depression. Expert Opin. Ther. Targets 8:7–14.

Heneka, M. T., M. Sastre, L. Dumitrescu-Ozimek, A. Hanke, I. Dewachter, C. Kuiperi, K. O'Banion, T. Klockgether, F. Van Leuven, and G. E. Landreth. 2005. Acute treatment with the PPARgamma agonist pioglitazone and ibuprofen reduces glial inflammation and Abeta1–42 levels in APPV717I transgenic mice. Brain 128:1442–53.

Iadecola, C., and M. Nedergaard. 2007. Glial regulation of the cerebral microvasculature. Nat. Neurosci. 10:1369–1376.

Kehoe, P. G., and G. K. Wilcock. 2007. Is inhibition of the renin-angiotensin system a new treatment option for Alzheimer's disease? Lancet Neurol. 6:373–378.

Klotz, L., M. Sastre, A. Kreutz, V. Gavrilyuk, T. Klockgether, D. L. Feinstein, M. T. Heneka. 2003. Noradrenaline induces expression of peroxisome proliferator activated receptor gamma (PPARgamma) in murine primary astrocytes and neurons. J. Neurochem. 86:907–916.

Korczyn, A. D., and V. Vakhapova. 2007. The prevention of the dementia epidemic. J. Neurol. Sci. 15:2–4.

Kovacs, T., N. J. Cairns, and P. L. Lantos. 1999. b-Amyloid deposition and neurofibrillary tangle formation in the olfactory bulb in ageing and Alzheimer's disease. Neuropathol. Appl. Neurobiol. 25:481–491.

Lacourcière, Y., J. M. Krzesinski, W. B. White, G. Davidai, H. Schumacher. 2004. Sustained antihypertensive activity of telmisartan compared with valsartan. Blood Press. Monit. 9:203–210.

Landreth, G. 2007. Therapeutic use of agonists of the nuclear receptor PPARgamma in Alzheimer's disease. Curr. Alzheimer Res. 4:159–164.

Lerner, A., and A. Bagic. 2008. Olfactory pathogenesis of idiopathic Parkinson disease revisited. Mov. Disord. 15:1076–1084.

Li, W., J. D. Howard, and J. A. Gottfried. 2010. Disruption of odour quality coding in piriform cortex mediates olfactory deficits in Alzheimer's disease. Brain 133:2714–2126.

Luna-Medina, R., M. Cortes-Canteli, M. Alonso, A. Santos, A. Martínez, and A. Perez-Castillo. 2005. Regulation of inflammatory response in neural cells in vitro by thiadiazolidinones derivatives through peroxisome proliferator-activated receptor gamma activation. J. Biol. Chem. 3:21453–21462.

Mogi, M., J. M. Li, K. Tsukuda, J. Iwanami, L. J. Min, A. Sakata, T. Fujita, M. Iwai, and M. Horiuchi. 2008. Telmisartan prevented cognitive decline partly due to PPAR-gamma activation. Biochem. Biophys. Res. Commun. 24:446–449.

Morales-Garcia, J. A., R. Luna-Medina, C. Alfaro-Cervello, M. Cortes-Canteli, A. Santos, J. M. Garcia-Verdugo, and A. Perez-Castillo. 2010. Peroxisome proliferator-activated receptor γ ligands regulate neural stem cell proliferation and differentiation in vitro and in vivo. Glia. 59:293–307.

Papademetriou, V. 2005. Hypertension and cognitive function. Blood pressure regulation and cognitive function: a review of the literature. Geriatrics 60:20–24.

Pearson, R. C., M. M. Esiri, R. W. Hiorns, G. K. Wilcock, and T. P. Powell. 1985. Anatomical correlates of the distribution of the pathological changes in the neocortex in Alzheimer's disease. Proc. Natl. Acad. Sci. USA 82:4531–4534.

Price, J. L. 2004. Olfactory system. Pp. 1197–1211 *in* G. R. Paxinos, ed. The human nervous system 2nd. Academic Press, New York.

Price, J. L., P. B. Davis, J. C. Morris, and D. L. White. 1991. The distribution of tangles, plaques and related immunohistochemical markers in healthy aging and Alzheimer's disease. Neurobiol. 12:295–312.

Saito, T., N. Iwata, S. Tsubuki, Y. Takaki, J. Takano, S. M. Huang, T. Suemoto, M. Higuchi, and T. C. Saido. 2005. Somatostatin regulates brain amyloid beta peptide Abeta42 through modulation of proteolytic degradation. Nat. Med. 11:434–439.

Saiz-Sanchez, D., I. Ubeda-Bañon, C. de la Rosa-Prieto, L. Argandoña-Palacios, S. Garcia-Muñozguren, R. Insausti, and A. Martinez-Marcos. 2010. Somatostatin, tau, and beta-amyloid within the anterior olfactory nucleus in Alzheimer disease. Exp. Neurol. 223:347–350.

Sakai, Y., H. Kumano, M. Nishikawa, Y. Sakano, H. Kaiya, E. Imabayashi, T. Ohnishi, H. Matsuda, A. Yasuda, and A. Sato. 2006. Changes in cerebral glucose utilization in patients with panic disorder treated with cognitive-behavioral therapy. Neuroimage 33:218–226.

Sastre, M., I. Dewachter, S. Rossner, N. Bogdanovic, E. Rosen, P. Borghgraef, B. O. Evert, L. Dumitrescu-Ozimek, D. R. Thal, and G. Landreth. 2006. Nonsteroidal anti-inflammatory drugs repress beta-secretase gene promoter activity by the activation of PPARgamma. Proc. Natl. Acad. Sci. USA 10:443–448.

Talairach, J., and P. Tournoux. 1988. Co-planar stereotactic atlas of the human brain. 1st ed. Thieme, Stuttgart, Germany. pp. 37–110.

Wada, K., A. Nakajima, K. Katayama, C. Kudo, A. Shibuya, N. Kubota, Y. Terauchi, M. Tachibana, H. Miyoshi, and Y. Kamisaki. 2006. Peroxisome proliferator-activated receptor gamma-mediated regulation of neural stem cell proliferation and differentiation. J. Biol. Chem. 5:12673–12681.

© 2011 The Authors. Published by Wiley Periodicals, Inc.

Wang, N., L. Verna, N. G. Chen, H. Li, B. M. Forman, and M. B. Stemerman. 2002. Constitutive activation of peroxisome proliferator-activated receptor-gamma suppresses pro-inflammatory adhesion molecules in human vascular endothelial cells. J. Biol. Chem. 13:34176–34181.

Watson, G. S., B. A. Cholerton, M. A. Reger, L. D. Baker, S. R. Plymate, S. Asthana, M. A. Fishel, J. J. Kulstad, P. S. Green, and D. G. Cook. 2005. Preserved cognition in patients with early Alzheimer disease and amnestic mild cognitive impairment during treatment with rosiglitazone: a preliminary study. Am. J. Geriatr. Psychiatry 13:950–958.

© 2011 The Authors. Published by Wiley Periodicals, Inc.

Published February 2, 2012 as 10.3174/ajnr.A2935

Automatic Voxel-Based Morphometry of Structural MRI by SPM8 plus Diffeomorphic Anatomic Registration Through Exponentiated Lie Algebra Improves the Diagnosis of Probable Alzheimer Disease

ORIGINAL RESEARCH

H. Matsuda
S. Mizumura
K. Nemoto
F. Yamashita
E. Imabayashi
N. Sato
T. Asada

BACKGROUND AND PURPOSE: The necessity for structural MRI is greater than ever to both diagnose AD in its early stage and objectively evaluate its progression. We propose a new VBM-based software program for automatic detection of early specific atrophy in AD.

MATERIALS AND METHODS: A target VOI was determined by group comparison of 30 patients with very mild AD and 40 age-matched healthy controls by using SPM. Then this target VOI was incorporated into a newly developed automated software program independently running on a Windows PC for VBM by using SPM8 plus DARTEL. ROC analysis was performed for discrimination of 116 other patients with AD with very mild stage (n = 45), mild stage (n = 30) and moderate-to-advanced stages (n = 41) from 40 other age-matched healthy controls by using a z score map in the target VOI.

RESULTS: Medial temporal structures involving the entire region of the entorhinal cortex, hippocampus, and amygdala showed significant atrophy in the patients with very mild AD and were determined as a target VOI. When we used the severity score of atrophy in this target VOI, 91.6%, 95.8%, and 98.2% accuracies were obtained in the very mild AD, mild AD, and moderate-to-severe AD groups, respectively. In the very mild AD group, a high specificity of 97.5% with a sensitivity of 86.4% was obtained, and age at onset of AD did not influence this accuracy.

CONCLUSIONS: This software program with application of SPM8 plus DARTEL to VBM provides a high performance for AD diagnosis by using MRI.

ABBREVIATIONS AD = Alzheimer disease; DARTEL = diffeomorphic anatomical registration through exponentiated lie algebra; FWHM = full width at half maximum; MCI = mild cognitive impairment; MMSE = Mini-Mental State Examination; ROC = receiver operating characteristic analysis; SPM = statistical parametric mapping; VBM = voxel-based morphometry

BRAIN

ORIGINAL RESEARCH

Increases in the number of individuals with dementia, the highest proportion of whom are affected by AD, have made early diagnosis of AD a major research and clinical priority. Of several neuroimaging techniques that provide surrogate markers for the diagnosis of AD, structural MRI is the most commonly used because of its noninvasiveness and excellent spatial resolution with good tissue contrast.[1] In AD, the earliest tissue loss occurs in the medial temporal structures, particularly in the entorhinal cortex.[2] However, visual inspection is insufficient for objective evaluation of mild atrophy. Although manual tracing of these structures can quantify the absolute volume, it is time-consuming and requires special expertise in anatomic knowledge for tracers. Recently, computer-aided VBM[3] has been applied to detect early atrophic changes in AD. Although this technique cannot provide the absolute volume, it can provide statistical results in comparisons of patients with AD with healthy controls.[4] Moreover VBM has been reported to be a surrogate indicator of the full brain topographic representation of the neurodegenerative aspect of AD pathology.[5] Hirata et al[6] proposed an automated software program, a voxel-based specific regional analysis system for AD, for the diagnosis of AD by using this VBM technique. In the present study, we revised this software by introducing new techniques and validated its utility.

Materials and Methods

A total of 251 subjects were studied in 1 center. We retrospectively chose 146 patients (65 men and 81 women) with a clinical diagnosis of probable AD according to the National Institute of Neurologic and Communicative Disorders and Stroke and the Alzheimer Disease and Related Disorders Association criteria.[7] These patients were classified into 3 groups of very mild, mild, and moderate-to-advanced AD. The very mild AD group comprised 75 patients (37 men and 38 women) who ranged in age from 51 to 86 years with a mean of 71.2 ± 7.4 years.

Received August 26, 2011; accepted after revision September 23.

From the Department of Nuclear Medicine (H.M., E.I.), Saitama Medical University International Medical Center, Hidaka, Saitama, Japan; Department of Radiology (S.M.), Toho University Omori Medical Center, Ota-ku, Tokyo, Japan; Department of Psychiatry (K.N., T.A.), Graduate School of Comprehensive Human Sciences, University of Tsukuba, Tsukuba, Ibaraki, Japan; Research Association for Biotechnology (F.Y.), Minato-ku, Tokyo, Japan; and Department of Radiology (N.S.), National Center Hospital, National Center of Neurology and Psychiatry, Kodaira, Tokyo, Japan.

This work was supported by a Grant-in-Aid for Scientific Research, Ministry of Education, Culture, Sports, Science and Technology, Japan (21591578).

Please address correspondence to Hiroshi Matsuda, MD, Department of Nuclear Medicine, Saitama Medical University International Medical Center, 1397-1, Yamane Hidaka, Saitama, Japan; e-mail: matsudah@saitama-med.ac.jp

Indicates open access to non-subscribers at www.ajnr.org

Indicates article with supplemental on-line tables.

http://dx.doi.org/10.3174/ajnr.A2935

Copyright 2012 by American Society of Neuroradiology.

At the initial visit, they had no apparent loss in general cognitive, behavioral, or functional status and corresponded to the criteria of the amnestic type of MCI[8] or 0.5 in the Clinical Dementia Rating.[9] The MMSE score ranged from 24 to 29 (mean, 25.7 ± 1.5). During the subsequent follow-up period of 2–6 years, the subjects showed progressive cognitive decline and eventually fulfilled the diagnosis of probable AD. The mild and moderate-to-advanced AD groups comprised 30 patients (8 men and 22 women, 71.4 ± 6.8 years of age) and 41 patients (20 men and 21 women, 71.3 ± 7.7 years of age), respectively. The MMSE score ranged from 20 to 25 (mean, 21.4 ± 1.3) and from 6 to 19; (mean, 15.0 ± 3.5) for the mild and moderate-to-advanced AD groups, respectively. Eighty-one of these patients with AD (48 very mild, 11 mild, and 22 moderate-to-advanced) underwent follow-up MRI studies at an interval of 1–4 years for, at most, 6 years (mean, 3.3 ± 1.2 years), and most patients in the very mild and mild AD groups moved to a more advanced group during the follow-up period. Consequently, the total of MRI studies was 89, 57, and 123 for the very mild, mild, and moderate-to-advanced AD groups.

Eighty age-matched control subjects (37 men and 43 women) were healthy volunteers with no memory impairment or cognitive disorders. They ranged in age from 54 to 86 years with a mean of 70.4 ± 7.8 years. Their performance was within normal limits both on the Wechsler Memory Scale–Revised and the Wechsler Adult Intelligence Scale–Revised. Their MMSE scores ranged from 26 to 30 (mean, 29.1 ± 1.2). They did not differ in age or education from the patients with AD. Additionally, 25 healthy volunteers (15 men and 10 women; mean, 31.1 ± 7.8 years of age) participated in this study for creation of a customized template for spatial normalization in the statistical image analysis. The ethics committee approved this study, and all subjects provided informed consent to participate. None of them had asymptomatic cerebral infarction detected by T2-weighted MRI.

All subjects underwent an MRI study on a 1.5T Vision Plus imager (Siemens, Erlangen, Germany). One hundred forty 3D sections of a T1-weighted magnetization-prepared rapid acquisition of gradient echo sequence were obtained in a sagittal orientation as 1.2-mm thick sections (FOV = 23, TR = 9.7 ms, TE = 4 ms, flip angle = 12°, and TI = 300 ms, with no intersection gaps).

First, to define a target VOI for early diagnosis of AD, we performed a group comparison between 30 patients (14 men and 16 women; mean age, 73.8 ± 4.8 years) randomly chosen in the present very mild AD group and the present 40 healthy controls group (19 men and 21 women; mean age, 70.8 ± 8.5 years). Using the latest version of SPM8 (Wellcome Department of Imaging Neuroscience, London, United Kingdom), we segmented MRIs into gray matter, white matter, and CSF images by a unified tissue-segmentation procedure after image-intensity nonuniformity correction. These segmented gray matter images were then spatially normalized to the customized template in the standardized anatomic space by using DARTEL (Wellcome Department of Imaging Neuroscience).[10] The customized template for DARTEL was created from the aforementioned 25 healthy young subjects. To preserve gray matter volume within each voxel, we modulated the images by the Jacobean determinants derived from the spatial normalization by DARTEL and then smoothed them by using an 8-mm FWHM Gaussian kernel. To compare the present analysis by using SPM8 plus DARTEL with the previously reported analysis,[6] we also defined a target VOI by using an old SPM version, SPM2 (Wellcome Department of Imaging Neuroscience) between the same 2 groups. Group comparisons by SPM were assessed by using the family-wise error at a threshold of $P < .05$, corrected for multiple comparisons.

A stand-alone software program running on Windows for VBM analysis by SPM8 plus DARTEL was developed to discriminate patients with AD from healthy controls. First, MRIs were spatially normalized with only a 12-parameter affine transformation to the SPM template so as to correct for differences in brain size. These linearly transformed images were nonlinearly transformed and then modulated to the customized template for DARTEL, followed by smoothing by using an 8-mm FWHM kernel. Each processed gray matter image of the remaining 116 patients with AD and 40 healthy controls was compared with the mean and SD of gray matter images of the 40 healthy volunteers chosen in the group comparison by using voxel-by-voxel z score analysis with and without voxel normalization to global mean intensities (global normalization): z score = ([control mean] − [individual value]) / (control SD). These z score maps were displayed by overlay on tomographic sections and surface rendering of the standardized brain. This program registered the target VOI defined by the aforementioned group comparison. This software program takes 8 minutes 40 seconds for all procedures by using a 64-bit PC with a Core i7 central processing unit and 6-gigabytes memory (Intel, Santa Clara, California).

We determined 4 indicators for characterizing atrophy in a target VOI and in the whole brain: first, the severity of atrophy obtained from the averaged positive z score in the target VOI; second, the extent of a region showing significant atrophy in the target VOI—that is, the percentage rate of the coordinates with a z value exceeding the threshold value of 2 in the target VOI; third, the extent of a region showing significant atrophy in the whole brain—that is, the percentage rate of the coordinates with a z value exceeding the threshold value of 2 in the whole brain; and fourth, the ratio of the extent of a region showing significant atrophy in the target VOI to the extent of a region showing significant atrophy in the whole brain. The utility of these indicators for this discrimination of AD from healthy controls has been reported in previous MRI[6] and SPECT studies.[11]

These 4 indicators were obtained under 2 conditions, with or without global normalization. Using the values of the 4 indicators as the threshold, we determined ROC curves for discrimination of patients with AD from healthy volunteers by using JMP 7.0 (SAS Institute, Cary, North Carolina). The program calculates the area under the ROC curves, sensitivity, specificity, and accuracy. Moreover, the age effects of AD onset on these 4 indicators and the results of the ROC were investigated in the very mild AD group classified into 2 subgroups with an age threshold of 65: the early-onset subgroup (16 patients, 9 men and 7 women; mean age, 58.0 ± 4.6 years) and the late-onset subgroup (29 patients, 14 men and 15 women; mean age, 73.8 ± 4.4 years).

Results

The group comparison by SPM8 plus DARTEL demonstrated significant decline of gray matter volume in the left (Talairach coordinates −24,−10,−14, x,y,z; z = 7.37 and 6.95 without and with global normalization, respectively) and the right (24,10,14, x,y,z; z = 7.42 and 7.05 without and with global normalization, respectively) parahippocampal gyri in patients with very mild AD (Fig 1). These bilateral regions involve the entorhinal cortex, head to tail of the hippocampus, and amygdala and are delineated as a target VOI for AD. Group comparison by SPM2 showed significant decline of gray matter volume in the left (−18, −7, −16, x,y,z; z = 6.18) and right

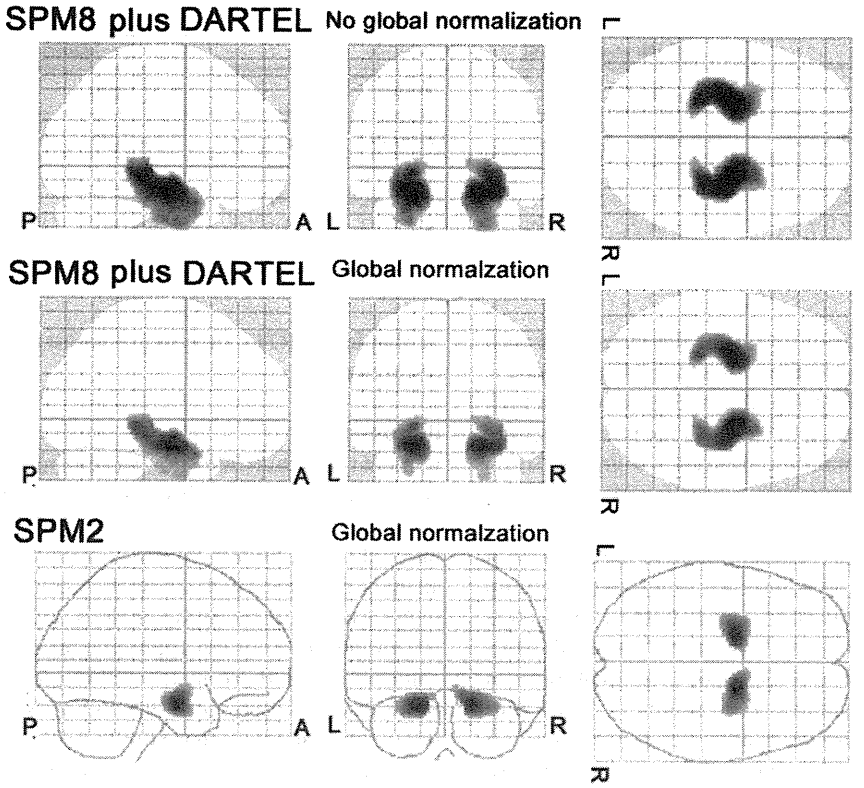

Fig 1. Group comparison of gray matter volume by SPM8 plus DARTEL and SPM2 between 30 patients with very mild AD and 40 healthy age-matched volunteers. The SPM8 plus DARTEL analysis demonstrates significant decline of gray matter volume in the bilateral medial temporal structures both with and without global normalization in patients with very mild AD. The cluster shape is very close to the anatomic configuration of the medial temporal structures involving the entorhinal cortex, amygdala, and hippocampal formation from head to tail. Although the SPM 2 analysis demonstrates a significant decline of gray matter volume in the bilateral medial temporal structures, the cluster is confined to the anterior parts of the medial temporal structures.

Table 1: Values of 4 indicators for characterizing atrophy[a]

		SPM8 plus DARTEL				SPM2			
		Target VOI			Whole-Brain	Target VOI			Whole-Brain
Group	Global Normalization	Severity	Extent (%)	Ratio	Extent (%)	Severity	Extent (%)	Ratio	Extent (%)
Healthy controls	−	0.7 ± 0.5	4.4 ± 9.8	0.8 ± 1.5	2.5 ± 4.7	NA	NA	NA	NA
	+	0.7 ± 0.3	2.0 ± 4.9	1.3 ± 2.8	1.4 ± 0.9	0.5 ± 0.3	1.8 ± 7.3	0.5 ± 1.8	2.6± 3.1
Very mild AD	−	1.8 ± 0.9[b]	39.0 ± 35.5[b]	9.9 ± 8.9[b]	5.4 ± 7.6[b]	NA	NA	NA	NA
	+	2.2 ± 0.9[b]	49.2 ± 30.2[b]	12.9 ± 7.8[b]	4.1 ± 2.5[b]	1.6 ± 1.0[b]	30.8 ± 32.1[b]	6.7 ± 7.8[b]	5.4 ± 3.7[b]
Mild AD	−	2.2 ± 0.7[b]	53.7 ± 29.8[b]	12.8 ± 8.8[b]	5.5 ± 5.1[b]	NA	NA	NA	NA
	+	2.7 ± 0.8[b]	63.7 ± 25.8[b]	15.4 ± 7.8[b]	4.3 ± 1.9[b]	2.1 ± 1.1[b]	42.0 ± 32.3[b]	9.6 ± 9.2[b]	5.4 ± 3.0[b]
Moderate-to-advanced AD	−	2.8 ± 1.0[b,c,d]	72.2 ± 26.5[b,c,d]	8.4 ± 7.2[b]	15.1 ± 14.0[b,c,d]	NA	NA	NA	NA
	+	3.0 ± 1.0[b,c]	68.7 ± 24.1[b,c]	11.7 ± 6.7[b,d]	7.1 ± 3.7[b,c,d]	2.6 ± 1.4[b,c]	56.3 ± 33.2[b,c]	7.6 ± 6.2[b]	9.0 ± 5.0[b,c,d]

Note:—NA indicates not applicable; +, presence; −, absence.
[a] Tukey honest significance test in each condition of global normalization.
[b] $P < .001$ versus healthy controls.
[c] $P < .001$ versus very mild AD group.
[d] $P < .001$ versus mild AD group.

(18, −5,15, x,y,z; $z = 5.86$) parahippocampal gyri (Fig 1). The cluster size was smaller in SPM2 than in SPM8 plus DARTEL.

The patients with AD showed significantly ($P < .001$, Tukey honest significance test) greater values than healthy controls in all 4 indicators in both SPM8 plus DARTEL and SPM2 analysis (Table 1). The mild AD group showed not significant but greater values of all 4 indicators than the very mild AD group. The moderate-to-advanced AD group showed significantly ($P < .001$) greater values of severity and extent for the target VOI and extent for the whole brain than the very mild AD group. In contrast, the ratio for the target VOI in the moderate-to-advanced AD group was lower than that in the mild AD group and almost equal to that in the very mild AD group. Global normalization in SPM8 plus DARTEL analysis elevated the severity and ratio for the target VOI and diminished the extent for the whole brain in all AD groups. The SPM2 analysis showed lower values in severity, extent, and ratio for a target VOI and greater values in extent for the whole brain than the SPM8 plus DARTEL analysis.

In the SPM8 plus DARTEL analysis, better ROC results were obtained in the condition with than without global normalization, particularly in specificity (On-line Table 1). Of the

Table 2: Values of 4 indicators in early- and late-onset subgroups in very mild AD

		SPM8 plus DARTEL				SPM2			
		Target VOI			Whole-Brain	Target VOI			Whole-Brain
Global Normalization	Onset	Severity	Extent (%)	Ratio	Extent (%)	Severity	Extent (%)	Ratio	Extent (%)
−	Early	1.5 ± 0.7	25.3 ± 31.1	3.8 ± 3.8	5.1 ± 4.9	NA	NA	NA	NA
−	Late	1.9 ± 0.9	43.8 ± 35.6	5.9 ± 8.4	11.6 ± 9.5	NA	NA	NA	NA
+	Early	1.9 ± 0.7	37.4 ± 26.2	9.5 ± 6.0	4.1 ± 1.7	1.4 ± 1.0	24.4 ± 34.6	4.7 ± 5.5	3.8 ± 2.4
+	Late	2.3 ± 0.9	53.6 ± 30.7	14.1 ± 8.1	4.1 ± 2.7	1.7 ± 1.0	33.2 ± 31.2	7.5 ± 8.5	6.0 ± 3.9

Note:—NA indicates not applicable; +, presence; −, absence.

4 indicators, the severity and extent for the target VOI with global normalization showed almost equal and high accuracy. Even in the very mild AD group, the severity showed a high accuracy of 91.6%, increasing to 95.8% in the mild AD group and 98.2% in the moderate-to-advanced AD group. SPM8 plus DARTEL showed better ROC results for all 4 indicators than SPM2.

Although the early-onset subgroup showed lower values of indicators for the target VOI than the late-onset subgroup (Table 2), global normalization elevated these indicators evenly in the early- and late-onset subgroups. These indicators were largely stable before and after global normalization in healthy controls. Consequently, ROC results in SPM8 plus DARTEL revealed equal accuracy after global normalization between these 2 subgroups (Online Table 2). In contrast, SPM2 analysis showed approximately 10% lower accuracy in the early-onset subgroup than that in the late-onset subgroup when using the severity score.

In each of 81 follow-up patients with AD, the severity score in a target VOI gradually increased from the baseline to follow-up studies. The annual increase of the severity score after global normalization was 0.27 ± 0.15.

Representative cross-sectional and longitudinal studies for SPM8 plus DARTEL analysis are demonstrated in Figs 2 and 3, respectively.

Discussion

Using severity as an indicator, we obtained a high sensitivity of 86.4% and extremely high specificity of 97.5%, resulting in an accuracy of 91.6% for discrimination of patients with very mild AD from healthy controls in the SPM8 plus DARTEL analysis. Extremely high specificity mainly contributed to this high accuracy. In the SPM2 analysis, ROC analysis presented 5% lower sensitivity and approximately 13% lower specificity compared with those in the SPM8 plus DARTEL analysis. Kawachi et al[12] reported 82.9% in both sensitivity and specificity in the patients with very mild AD in a similar VBM study by using an older SPM version, SPM99. This better specificity may result from application of the SPM8 plus DARTEL algorithm. This DARTEL algorithm can provide more precise spatial normalization to the template than the conventional algorithm.[10,13]

This improvement in the preciseness of the spatial normalization was confirmed by group comparison for determining a target VOI. The SPM8 plus DARTEL results showed significantly decreased volume with anatomically precise configura-

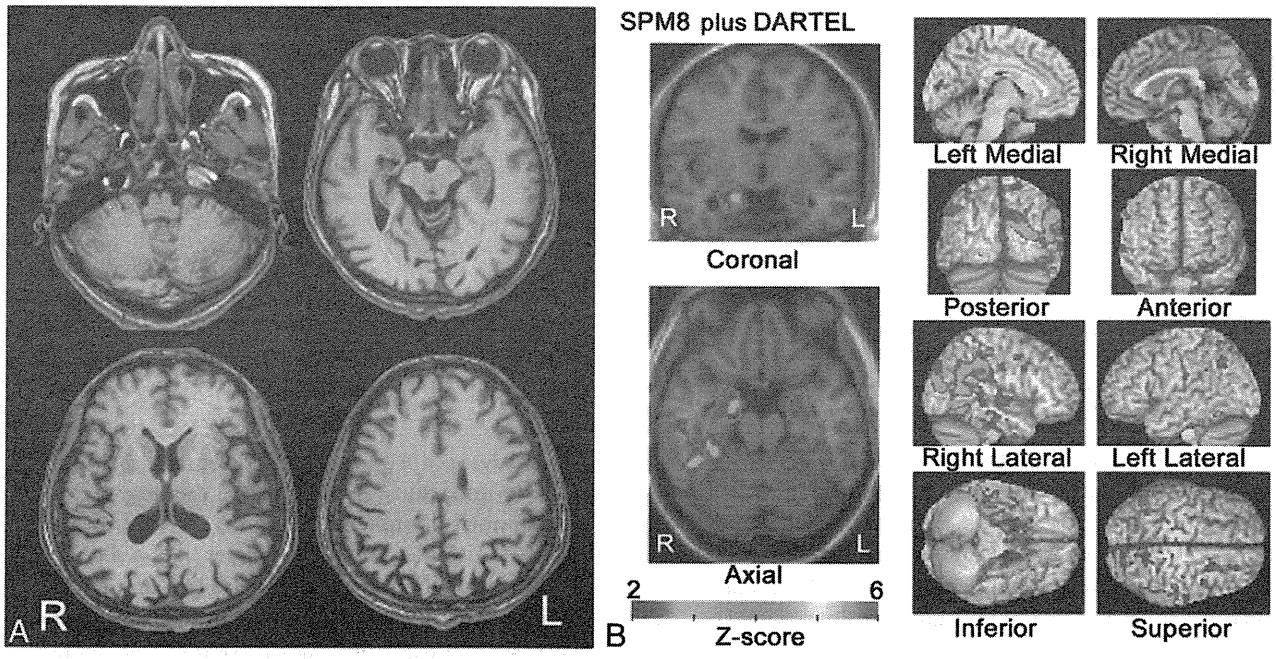

Fig 2. Cross-sectional VBM study by using SPM8 plus DARTEL. *A*, MR image of a 52-year-old woman with an MMSE score of 27. One year later the MMSE score declined to 19. *B*, SPM8 plus DARTEL analysis with global normalization reveals a significant decrease of gray matter volume in the right entorhinal area. Colored areas with *z* scores of >2 are overlaid as significantly atrophied regions on tomographic sections and cortical surface of the standardized MRI template. A target VOI in the medial temporal structures is demarcated with purple lines. The right temporoparietal cortex also shows extensive significant atrophy.

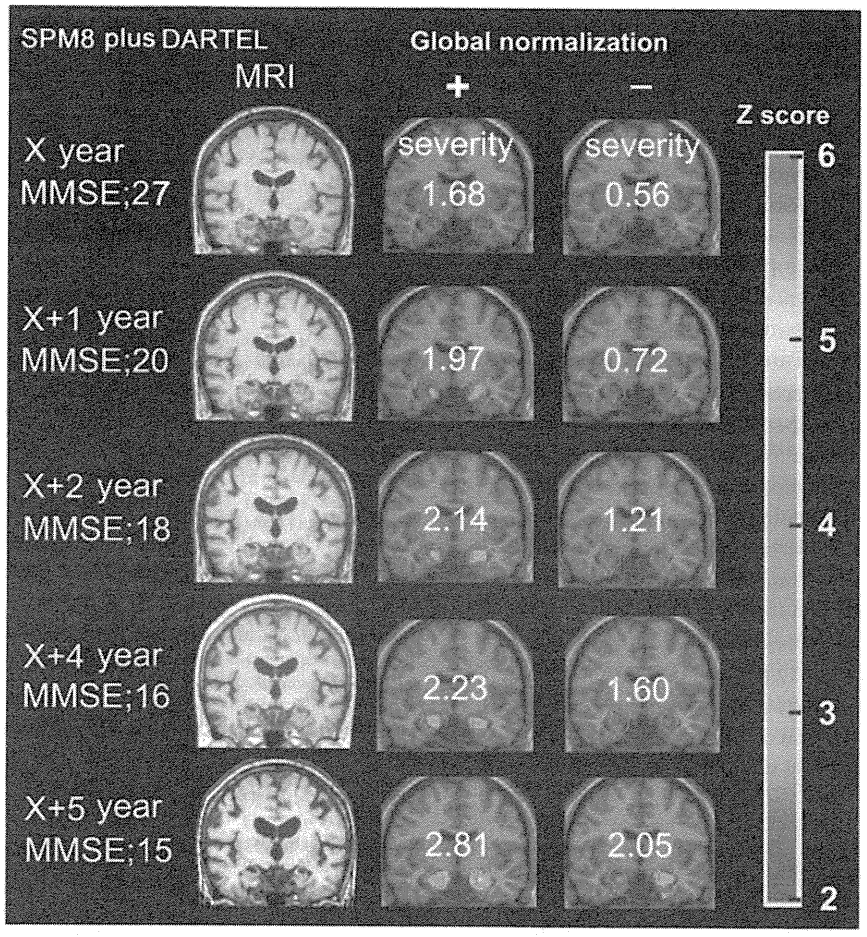

Fig 3. Longitudinal VBM studies by using SPM8 plus DARTEL. A 63-year-old woman with an MMSE score of 27 at the first visit was followed up for 6 years. One year later, the MMSE score decreased to 20 and gradually decreased thereafter. VBM analysis with global normalization reveals significant atrophy in the bilateral medial temporal areas even at the time of the initial study. Then the *z* score in a target VOI increased step by step with time. In contrast, analysis without global normalization does not demonstrate significant atrophy in the medial temporal areas for the first 3 years. Severity scores as an indicator for characterizing atrophy in the medial temporal structures are shown.

tion of the medial temporal structures involving the entorhinal cortex, amygdala, and total hippocampal formation. Takahashi et al[14] demonstrated almost identical results by using SPM8 plus DARTEL. The present SPM results by using conventional VBM by SPM2 showed decreased gray matter volume mainly in the anterior parts of the parahippocampal gyri with a less precise configuration. The severity score proved to be useful for longitudinal studies as well. The annual increase of this score may be indicative of disease progression.

The modulation in VBM allows comparison of the absolute amount of gray matter.[15] The step of global normalization allows correction of the absolute amount of gray matter for individual total brain volume. Comparison of discrimination performance demonstrated better results in the condition with than without global normalization. This difference in discrimination performance may arise from the well-known fact of selective atrophy in the medial temporal structures in AD.[1,4-6,16,17] Even if the absolute amount of gray matter of the medial temporal structures is decreased, a concomitant decrease in the total volume of gray matter would decrease specificity. The specificity in ROC analysis of the severity for the target VOI was 17% lower in the condition without than with global normalization in very mild AD. The degree of selective atrophy in the medial temporal areas can be assessed by the ratio as an indicator. In patients with AD, more than 10-fold selective atrophy was observed in the medial temporal areas compared with the whole brain in SPM8 plus DARTEL. Global normalization enhanced this ratio. Progression of neocortical atrophy would result in the decline of this ratio in advanced AD. This indicator may be useful for differentiation of AD from other neuropsychiatric diseases manifesting dementia.

The early-onset subgroup showed milder atrophy in the medial temporal structures than the late-onset subgroup. This is in line with several previous reports in which late-onset subgroups showed greater atrophy in the medial temporal structures than the early-onset subgroups.[16,17] However global normalization in SPM8 plus DARTEL extended the difference of indicators for a target VOI evenly in the early-onset and late-onset subgroups from indicators in healthy controls. This extension led to almost equal accuracy for discrimination of early-onset and late-onset very mild AD from healthy controls. This global normalization procedure may make it possible to use a common target VOI irrespective of age at onset of AD.

Thus the present study made it clear that the global normalization procedure in VBM by using SPM8 plus DARTEL has advantages in enhancing the discrimination power of diagnosing AD. However lower values of the extent for the whole brain after global normalization would underestimate neocor-

tical atrophy. The extent for the whole brain without global normalization may be useful for accurately evaluating the degree of neocortical atrophy.

This study is not without limitations. First, we should investigate whether this 1-site study is applicable to multicenter studies. Second, evaluation of the reproducibility of the present VBM technique may be necessary for longitudinal studies. Third, we investigated patients with amnestic MCI who all converted to AD. The outcome for any patient with MCI is uncertain because many subjects remain stable or even revert to a normal state, while others progress to dementia. Accordingly, the predictive study by using this VBM approach is much more important for MCI conversion to AD. Fourth, the single target VOI was used irrespective of age at onset of AD. A similar VBM study by Ishii et al[18] recommended the use of a target VOI involving not only medial temporal structures but also parietal and posterior cingulate cortices and precunei in early-onset AD. Although this software program presented the same accuracy between early- and late-onset very mild AD subgroups, we may have to investigate a more appropriate target VOI from a larger number of patients with early-onset AD. However, incorporation of 2 types of target VOIs for early- and late-onset AD into a software program may confound the program user in the selection of a target VOI in the case of follow-up studies on an approximately 65-year-old patient.

Conclusions

We proposed an automatic VBM software program of structural MRI for discrimination between patients with probable AD from the very-mild- to advanced stages and age-matched healthy controls. Application of the SPM8 plus DARTEL analysis to this software program provided a high accuracy of 91.6% for discrimination of patients with very mild AD from healthy controls by using a target VOI located in medial temporal structures. Equal accuracies were obtained in early-onset and late-onset very mild AD subgroups. This software program may be useful for early diagnosis and longitudinal evaluation of AD.

References

1. Frisoni GB, Fox NC, Jack CR Jr, et al. **The clinical use of structural MRI in Alzheimer disease.** *Nat Rev Neurol* 2010;6:67–77
2. Gómez-Isla T, Price JL, McKeel DW Jr, et al. **Profound loss of layer II entorhinal cortex neurons occurs in very mild Alzheimer's disease.** *J Neurosci* 1996;16:4491–500
3. Ashburner J, Friston KJ. **Voxel-based morphometry: the methods.** *Neuroimage* 2000;11:805–21
4. Baron JC, Chételat G, Desgranges B, et al. **In vivo mapping of gray matter loss with voxel-based morphometry in mild Alzheimer's disease.** *Neuroimage* 2001;14:298–309
5. Whitwell JL, Josephs KA, Murray ME, et al. **MRI correlates of neurofibrillary tangle pathology at autopsy: a voxel-based morphometry study.** *Neurology* 2008;71:743–49
6. Hirata Y, Matsuda H, Nemoto K, et al. **Voxel-based morphometry to discriminate early Alzheimer's disease from controls.** *Neurosci Lett* 2005;382:269–74
7. McKhann G, Drachman D, Folstein M, et al. **Clinical diagnosis of Alzheimer's disease: report of the NINCDS-ADRDA work group under the auspices of Department of Health and Human Services taskforce on Alzheimer's disease.** *Neurology* 1984;34:939–44
8. Petersen RC, Doody R, Kurz A, et al. **Current concepts in mild cognitive impairment.** *Arch Neurol* 2001;58:1985–92
9. Hughes CP, Berg L, Danziger WL, et al. **A new clinical scale for the staging of dementia.** *Br J Psychiatry* 1982;140:566–72
10. Ashburner J. **A fast diffeomorphic image registration algorithm.** *Neuroimage* 2007;38:95–113
11. Matsuda H, Mizumura S, Nagao T, et al. **Automated discrimination between very early Alzheimer disease and controls using an easy Z-score imaging system for multicenter brain perfusion single-photon emission tomography.** *AJNR Am J Neuroradiol* 2007;28:731–36
12. Kawachi T, Ishii K, Sakamoto S, et al. **Comparison of the diagnostic performance of FDG-PET and VBM-MRI in very mild Alzheimer's disease.** *Eur J Nucl Med Mol Imaging* 2006;33:801–09
13. Pereira JM, Xiong L, Acosta-Cabronero J, et al. **Registration accuracy for VBM studies varies according to region and degenerative disease grouping.** *Neuroimage* 2010;49:2205–15
14. Takahashi R, Ishii K, Miyamoto N, et al. **Measurement of gray and white matter atrophy in dementia with Lewy bodies using diffeomorphic anatomic registration through exponentiated lie algebra: a comparison with conventional voxel-based morphometry.** *AJNR Am J Neuroradiol* 2010;31:1873–78
15. Karas GB, Burton EJ, Rombouts SA, et al. **A comprehensive study of gray matter loss in patients with Alzheimer's disease using optimized voxel-based morphometry.** *Neuroimage* 2003;18:895–907
16. Matsunari I, Samuraki M, Chen WP, et al. **Comparison of 18F-FDG PET and optimized voxel-based morphometry for detection of Alzheimer's disease: aging effect on diagnostic performance.** *J Nucl Med* 2007;48:1961–70
17. Frisoni GB, Pievani M, Testa C, et al. **The topography of grey matter involvement in early and late onset Alzheimer's disease.** *Brain* 2007;130:720–30
18. Ishii K, Kawachi T, Sasaki H, et al. **Voxel-based morphometric comparison between early- and late-onset mild Alzheimer's disease and assessment of diagnostic performance of z score images.** *AJNR Am J Neuroradiol* 2005;26:333–40

Review
Clinical Psychopharmacology and Neuroscience 2011;9(1):9-16

pISSN 1738-1088 / eISSN 2093-4327
Copyright©2011, Korean College of Neuropsychopharmacology

Central Nervous System Drug Evaluation Using Positron Emission Tomography

Mizuho Sekine[1,2], Jun Maeda[1], Hitoshi Shimada[1], Tsuyoshi Nogami[1,2], Ryosuke Arakawa[1,2], Harumasa Takano[1], Makoto Higuchi[1], Hiroshi Ito[1], Yoshiro Okubo[2], Tetsuya Suhara[1]

[1]Molecular Neuroimaging Group, Molecular Imaging Center, National Institute of Radiological Sciences, Chiba, [2]Department of Neuropsychiatry, Nippon Medical School, Tokyo, Japan

In conventional pharmacological research in the field of mental disorders, pharmacological effect and dose have been estimated by ethological approach and in vitro data of affinity to the site of action. In addition, the frequency of administration has been estimated from drug kinetics in blood. However, there is a problem regarding an objective index of drug effects in the living body. Furthermore, the possibility that the concentration of drug in blood does not necessarily reflect the drug kinetics in target organs has been pointed out. Positron emission tomography (PET) techniques have made progress for more than 20 years, and made it possible to measure the distribution and kinetics of small molecule components in living brain. In this article, we focused on rational drug dosing using receptor occupancy and proof-of-concept of drugs in the drug development process using PET.

KEY WORDS: Positron emission tomography; Occupancy; Dopamine D_2 receptor; Serotonin transporter; Norepinephrine transporter; micro-PET.

INTRODUCTION

In conventional pharmacological research in the field of mental disorders, pharmacological effect and dose have been estimated by ethological approach and in vitro data of affinity to the site of action. In addition, the frequency of administration has been estimated from drug kinetics in blood. However, there is a problem regarding an objective index of drug effects in the living body. Furthermore, the possibility that the concentration of drug in blood does not necessarily reflect the drug kinetics in target organs has been pointed out. Positron emission tomography (PET) techniques have made progress for more than 20 years, and made it possible to measure the distribution and kinetics of small molecule components in living brain, PET neuroimaging including neuroreceptor imaging and enzyme activity imaging have contributed to drug evaluation by 1) rational drug dosing, 2) biodistribution of drug, 3) therapeutic rationale for drug utilization, and 4) mechanism of drug action.[1)] In this article, we focused on rational drug dosing using receptor occupancy and proof-of-concept of drugs in the drug development process using PET.

Received: October 31, 2010 / **Revised:** January 18, 2011
Accepted: January 19, 2011
Address for correspondence: Mizuho Sekine, MD, PhD
Molecular Neuroimaging Group, Molecular Imaging Center, National Institute of Radiological Sciences, 4-9-1, Anagawa, Inage-ku, Chiba, 263-8555, Japan
Tel: +81-43-206-3251, Fax: +81-43-253-0396
E-mail: sekine@nirs.go.jp

Dopamine D_2 Receptor Occupancy by Antipsychotics

Dopamine dysregulation has been suspected for the pathophysiology of schizophrenia. The common pharmacological profile of antipsychotics that can alleviate positive symptoms has a dopamine D_2 receptor blocking property.[2)] Farde and others succeeded in visualizing dopamine D_2 receptors by using the selective, high-affinity dopamine D_2 receptor antagonist ^{11}C-labeled raclopride and PET, allowing estimation of dopamine D_2 receptor bindings quantitatively in the human brain.[3)] By applying this technique, it was possible to evaluate the degree of dopamine D_2 receptor inhibition of antipsychotics as a change of radioligand binding. Using a binding potential (BP) reflecting the receptor density at the specific binding site,occupancy was defined as the percentage reduction of BP and calculated as follows:

$$Occupancy(\%) = \frac{BP_{baseline} - BP_{drug}}{BP_{baseline}} \times 100$$

There are some reports concerning dopamine D_2 receptor occupancy by antipsychotics in living human brain. A range of 70 to 89% was reportedin an open study of 22

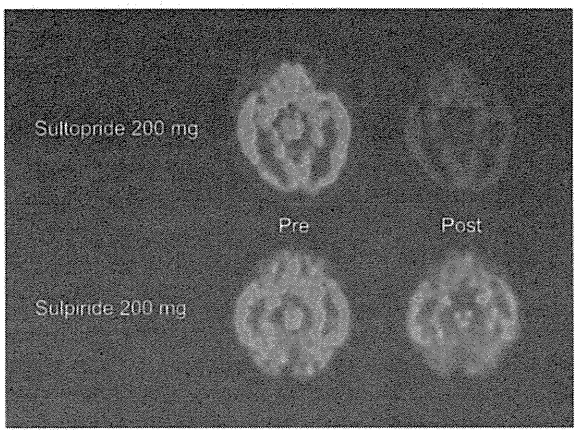

Fig. 1. Typical summated PET images before and after administration of 200mg of Sultopride and Sulpiride.[13] (upper stand) Pre is typical summated PET image before sultopride administration. Post is typical summated PET image at the possible peak time of plasma concentration of the sultopride, 2 hr after single administration of 200 mg of sultopride. (lower stand) Pre is typical summated PET image before sulpiride administration. Post is typical summated PET image at the possible peak time of plasma concentration of the sulpiride, 3 hr after single administration of 200 mg of sulpiride. The absolute decline in dopamine D_2 binding is significantly greater after administration of sultpride than sulpiride. PET, positron emission tomography.

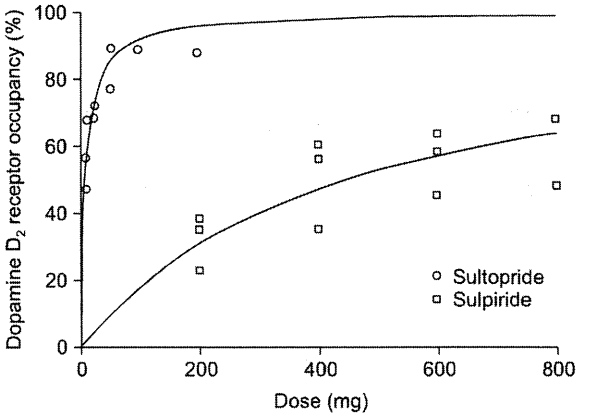

Fig. 2. Relationship between dopamine D_2 receptor occupancy and doses of sulpiride and sultopride.[13] Mean dopamine D_2 receptor occupancy of three regions (prefrontal cortex, temporal cortex, and thalamus) was shown as dopamine D_2 receptor occupancy. Open squares indicate sulpiride, and open circles indicate sultopride. The dotted regression curve was fitted to the sulpiride data, and the solid regression curve was fitted to the sultopride data.

schizophrenic patients responding to treatment with conventional doses of classical neuroleptics.[4] A double-blind PET study of schizophrenic patients suggested that dopamine D_2 receptor occupancywas positively correlated with the percentage of reduction in total Brief Psychopathological Rating Scale (BPRS) score at the end of treatment compared to baseline, and the dopamine D_2 receptor occupancy valuerequired to induce 50% reduction of BPRS was about 70%.[5] Another double-blind PET study reported a significant relationship between dopamine D_2 receptor occupancy and improvement in Clinical Global Impressions Scale (CGI) rating, with over 65% dopamine D_2 receptor occupancy showing a distinct clinical response.[6] On the basis of these findings, the likelihood of clinical response increases as dopamine D_2 receptor occupancy exceeds 70%, while the risks of extrapyramidal symptoms (EPSs) increase at occupancy higher than 80%.

Dose-finding of Antipsychotics Based on Dopamine D_2 Receptor Occupancy

Appropriate dosages of various antipsychotics are now being decidedbased on measurements of dopamine D_2 receptor occupancy. Previous studies reported that a dose range between 3 and 5 mg/day of risperidone was assumed to be optimal for supporting the clinical outcome.[7,8] Moreover, the appropriate dosage of olanzapine has been reported to be 8-14 mg/day, also in good agreement with the clinical dose.[9,10] In a phase II clinical trial in Japan, paliperidone ER at 6-9mg/day provides an estimated level of dopamine D_2 receptor occupancy between 70-80% .[11] In Korea as well, dopamine D_2 receptor occupancy by a novel antipsychotic, YKP1358, was measured using PET,[12] and this will require further clinical study.

Thus, performing a dose-finding study using PET at the clinical trial stage has been considered one of the reasons for the fewer side effects of the so-called second-generation antipsychotics.

On the other hand, in terms of conventional antipsychotics, there have not been enough supporting data regarding clinical doses based on dopamine D_2 receptor occupancy. Takano and others measured dopamine D_2 receptor occupancy of two conventional benzamide antipsychotics, sulpiride and sultopride, using positron emission tomography, to investigate the rationale of their clinical doses.[13] In that study, doses required for 70-80% occupancy were shown to be quite different: 1,010-1,730 mg for sulpiride but 20-35 mg for sultopride despite their similar registered clinical doses (300-1,200 mg) (Fig. 1, 2). Sultopride has been reported to induce more EPSs than sulpiride, which can be attributed to the fact that the registered clinical doses of sultopride were approximately 10 times higher than the calculated optimal doses.

As evidence for the clinical doses of conventional antipsychotics has been limited, their re-evaluation based on dopamine D_2 receptor occupancy can contribute to the es-

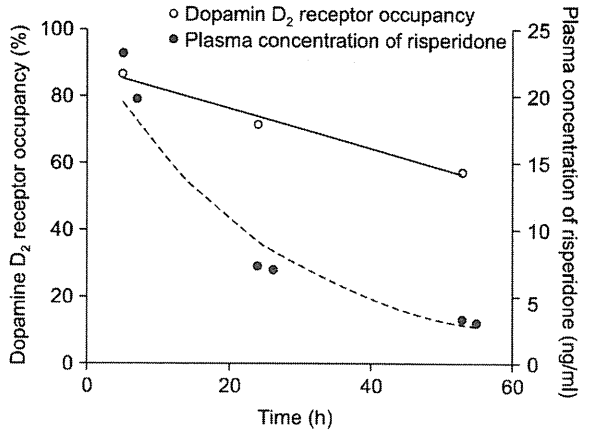

Fig. 3. Time-course of D_2 receptor occupancy by risperidone.[17] Time-course of dopamine D_2 receptor occupancy in the temporal cortex (●) and the plasma concentrations (○) after taking 4 mg risperidone. The sum of the plasma concentrations of risperidone and 9-OH-risperidone was used as the plasma concentration of risperidone. The $T_1/_2$ of plasma concentration (17.7 h) was shorter than that of dopamine D_2 receptor occupancy (73.8 h).

tablishment of rational antipsychotic therapy.

Although the concept of a "therapeutic window" between 70-80% of dopamine D_2 receptor occupancy seems to apply for most antipsychotics, there may be a different optimal occupancy other than 70-80% depending on the characteristic of drugs such as aripiprazole, dopamine D_2 receptor partial agonist, occupy more than 90% of striatal dopamine D_2 receptor at clinically effective doses.[14,15] Furthermore, optimal occupancy of low-affinity drugs such as clozapine and quetiapine have been inconclusive.[16]

Pharmacokinetics at Specific Binding Site

Until now, drug disposition has been mainly evaluated by plasma kinetics. However, it is important to directly focus on the kinetic profile at the specific binding site, except for the drugs that have a site of action in blood. Therefore, the time-course of occupancy at the binding site of the drug reflects the drug kinetics at the specific binding site, and is an important index. Takano and others measured the time-course of dopamine D_2 receptor occupancy in the temporal cortex as well as that of risperidone plasma concentration after its administration in chronically treated patients.[17] The half-life of the plasma concentration (17.7 h) was shorter than that of dopamine D_2 receptor occupancy (73.8 h) (Fig. 3). Furthermore, they reported that the estimated time-course of dopamine D_2 receptor occupancy from the mean pharmacokinetics data and the in-vivo ED_{50} value fitted well with the data from consecutive PET scans. Thus, estimating the drug kinetics at the receptor site in this way can applicable to appropriate dose scheduling.

Regionality of dopamine D_2 Receptor Occupancy

The concept of limbic and cortical selectivity of second-generation antipsychotics, i.e., higher dopamine D_2 receptor occupancy in the cerebral cortices than in the striatum, has also been suggested to explain their clinical efficacy with few EPSs.[18] Limbic and cortical selectivity was originally observed in dopamine D_2 receptor occupancy by clozapine in patients with schizophrenia using [^{123}I]epidepride.[18] Limbic and cortical selectivity was also reported in other second-generation antipsychotics such as risperidone and olanzapine.[19,20] However, in most studies concerning the regional selectivity of dopamine D_2 receptor occupancy in patients with schizophrenia, baseline binding to receptors for the calculation of occupancy was based on binding of other healthy subjects, not the binding of the neuroleptic-naive state of the same patients. In addition, dopamine D_2 receptor density is quite different between striatal and extrastriatal regions. Therefore, to elucidate the regional difference in dopamine D_2 receptor occupancy by second-generation antipsychotics, Ito and others measured dopamine D_2 receptor occupancy in the striatal and extrastriatal regions by different tracers with different affinity for receptors using the neuroleptic-naive state of the same subjects as the baseline. No obvious regional differences in dopamine D_2 receptor occupancy by risperidone were observed.[21] Moreover, dopamine D_2 receptor occupancy in the extrastriatal region by olanzapine has also been reported to agree with occupancy in the striatum.[9] By adapting an appropriate measurement in this way, it could be shown that the concept of limbic and cortical selectivity of risperidone and olanzapine was not observed.

Dopamine D_2 Receptor Occupancy in the Pituitary

Hyperprolactinemia, one of the common side effects of antipsychotic drugs, is reported to be induced by blocking of dopamine D_2 receptors in the pituitary. Although examination of the relation between dopamine D_2 receptor occupancy and hyperprolactinemia has been attempted using PET,[6,22,23] the outcomes have been inconclusive. Arakawa and others reported that the dopamine D_2 receptor occupancy in the pituitary by 4 antipsychotic drugs was significantly correlated with the plasma concentration of prolactin, but no such correlation was found in the temporal cortex (Fig. 4).[24] Furthermore, a character-

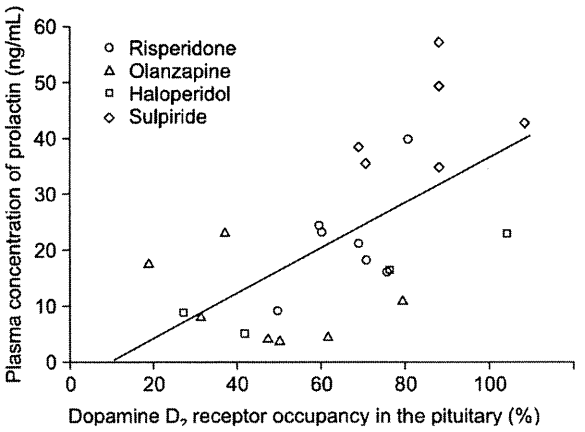

Fig. 4. Relation between plasma concentration of prolactin and dopamine D_2 receptor occupancy in the pituitary.[24] Significant positive correlation was observed between the plasma concentration of prolactin and dopamine D_2 receptor occupancy in the pituitary by different doses of risperidone, olanzapine, haloperidol, and sulpiride (Y=0.41; X-4.0; p=.001).

istic tendency of each drug was observed in dopamine D_2 receptoroccupancy in the pituitary and the temporal cortex. Sulpiride, known to be prone to hyperprolactinemia, blocked dopamine D_2 receptors in the pituitary more preferentially than in the temporal cortex, whereas olanzapine showed relatively less occupied dopamine D_2 receptors in the pituitary. This is due to the fact that the pituitary exists outside the blood-brain barrier. The magnitude of hyperprolactinemia of various antipsychotics can be predicted by the permeability of each antipsychotic into the brain. Thus, especially in the area of new drug development, the permeability of each antipsychotic drug might prove to be useful for the early evaluation of the risk of hyperprolactinemia.

Serotonin Transporter Occupancy by Antidepressant

Serotonin transporters (5-HTT) are located at presynaptic serotonergic neurons and have a key role in the regulation of serotonin concentration in the synapse. They are believed to be one of the major therapeutic targets of antidepressants. PET studies, using radioligands such as [^{11}C]McN(+)5652 and [^{11}C]DASB, have made it possible to measure the occupancy of 5-HTT by antidepressants in living human brain. 5-HTT occupancy was reported to be over 80% at clinical doses of selective serotonin reuptake inhibitors (SSRIs) during the treatment of depression.[25,26] Suhara and others investigated the relationship between 5-HTT occupancy and the dose of the classic tricyclic antidepressant (TCA) clomipramine, and one of the SSRIs, fluvoxamine.[26] In this study, even 10 mg of clomipramine showed approximately 80% 5-HTT occupancy, while step-wise increases of fluvoxamine in dosage demonstrated only a gradual increase (Fig. 5). In a dose-finding study of duloxetine, a part of phase I clinical trials in Japan, it was reported that 40mg or more was needed to attain 80% occupancy, and 60 mg of duloxetine could maintain a high level of 5-HTT occupancy with a once-a-day administration schedule.[27]

However, a distinct threshold in 5-HTT occupancy for achieving an antidepressant effect without side effects, comparable to dopamine D_2 receptor occupancy by antipsychotics, has not yet been demonstrated. Additionally, clomipramine, its metabolite desmethyl-clomipramine and duloxetine have affinity to norepinephrine transporter (NET) as well as 5-HTT. Although evaluation of NET occupancy is required, suitable radioligands for NETwere not developed at the time these studies were carried out.

Norepinephrine Transporter Occupancy by Antidepressant

Norepinephrine, one of the monoamine neurotransmitters in the central nervous system, has been reported to be related to several functions such as memory, cognition, consciousness, emotion, etc. NET is responsible for the reuptake of norepinephrine into pre-synaptic nerves and is another main target of antidepressants such as serotonin-norepinephrine reuptake inhibitors (SNRIs) and TCAs. SSRIs are widely considered as the first choice of treatment for depression. However, it is known that about one-third of the patients with major depression do not respond to SSRIs.[28,29] Recent studies have suggested that the treatment of depression with newer antidepressants that simultaneously enhance both serotonergic and norepinephrinergic neurotransmissions can be expected to result in higher response and remission rates compared to SSRIs.[30,31] Therefore, examining NET occupancy by TCAs and SSRIs might provide a new therapeutic indication other than 5-HTT occupancy.

As mentioned above, several studies have been reported regarding 5-HTT occupancy by antidepressants. However, NET occupancy by antidepressants in human brain has not been reported because of a lack of suitable radioligands for NET. (S,S)-[^{18}F]FMeNER-D_2 was recently developed as a radioligand for the measurement of NET binding with PET,[32] allowing estimation of NET bindings quantitatively in human brain.[33-35] Furthermore, NET occupancy by nortriptyline, corresponding to the administration dose and plasma concentration of nortriptyline, was observed in human brain using PET with

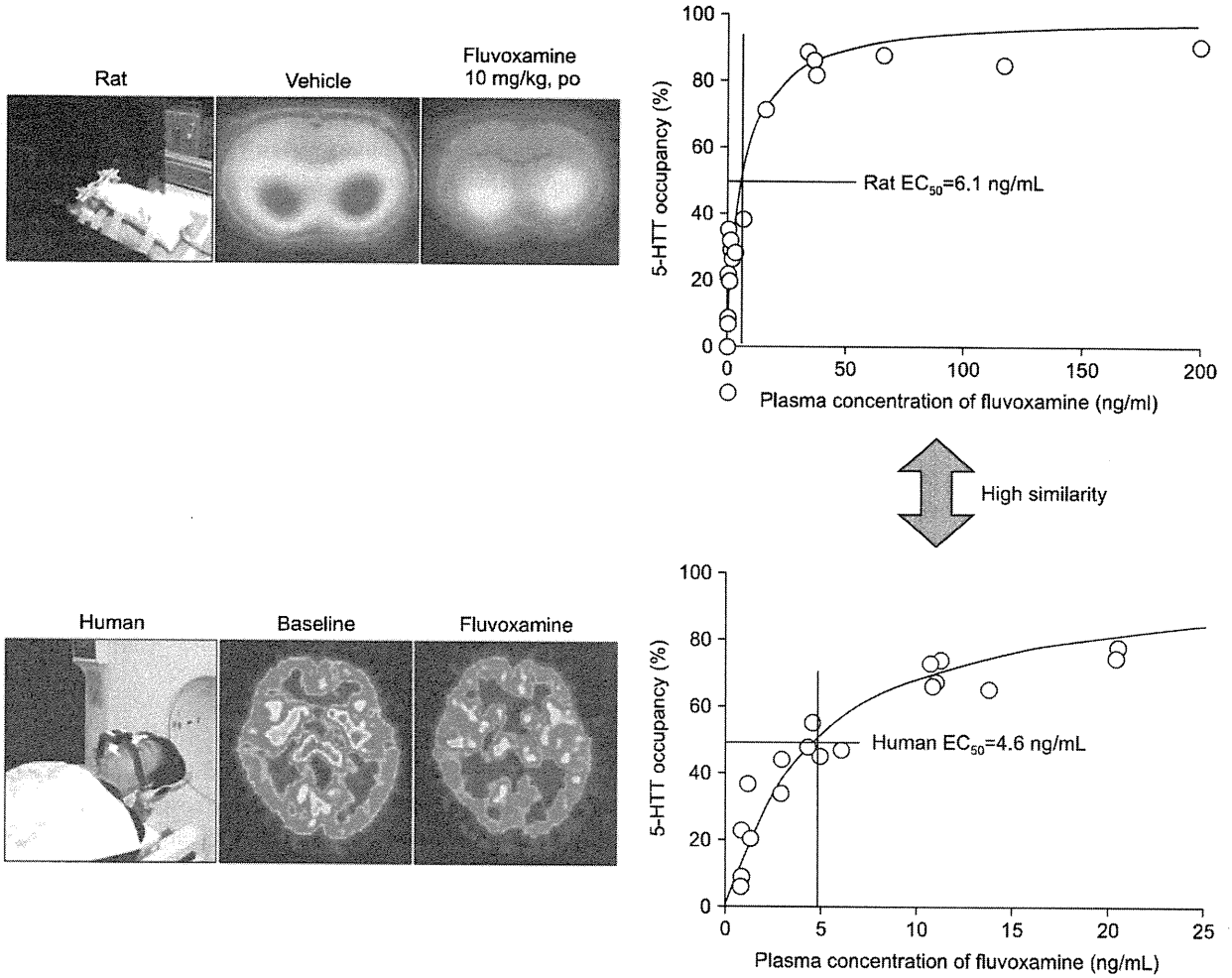

Fig. 5. Serotonin transporter occupancy by SSRI fluvoxamine in rat[45] and human brain.[47] (left side) PET imaging of (^{11}C)DASB distribution in rat and human brain before and after oral administration of fluvoxamine. (right side) Relationship between plasma concentration of fluvoxamine and 5-HTT occupancy in rat and human brain. The plasma concentration of fluvoxamine needed for 50% occupancy (EC_{50}=6.1 ng/ml) was almost equivalent to the value determined in human studies (EC_{50}=4.6 ng/ml).

(S,S)-[^{18}F]FMeNER-D_2.[36] Further NET occupancy studies in humans will be needed to evaluate the relation with the clinical effects of antidepressants.

Biomarkers for the Proof-of-Concept of Drugs and New Treatments

The most utilized imaging biomarker for rational drug dosing is the receptor or transporter occupancy by drugs acting on those sites as blockers. However, in psychiatric disorders, reliable diagnostic biomarkers are still awaited. Nonetheless, in the case of Alzheimer disease (AD), distinctive pathological changes such as deposition of β-amyloid protein (Aβ) and neurofibrillary tangles (NFT) have been identified. Quantification of Aβ in living human brain is reported to represent an important diagnostic biomarker for AD. Several amyloid ligands, such as [^{11}C]PIB, [^{11}C]BF227, [^{11}C]AZD-2184 and [^{18}F]AV-45, have been developed for PET imaging.[37-41]

Furthermore, Rinneand others reported that cortical [^{11}C]PIB retention was reduced in the AD patients group received the treatment with bapineuzumab, a humanised anti-Aβ monoclonal antibody, compared with both baseline and the placebo group.[42] Measurement of brain Aβ deposition by PET may be useful not only for early diagnosis of AD but also for therapeutic monitoring of the effects of disease-modifying agents such as anti-Aβ monoclonal antibody, secretase inhibitors or modifiers, metal-protein attenuating compounds, antioxidants and so on. Despite the distinctive biomarker and several promising therapeutic agents, current treatment of AD is limited to

the enhancement of acetylcholinergic neurotransmission. This treatment is based on the pathology of a reduction in acetylcholinergic neurotransmission, thought to be responsible for several symptoms including memory impairment. Although an acetylcholinesterase inhibitor such as donepezil hydrochloride is assumed to increase the synaptic acetylcholine level, direct evidence of the mechanism of its action in the living human brain was needed. Using PET and radiolabeled acetylcholine analogue [^{11}C]N-methyl-4-piperidyl acetate (MP4A), also a substrate of acetylcholinesterase, and 5 mg of donepezil hydrochloride, acetylcholinesterase activity was reported to be reduced by 34.6% in AD brain.[43]

Translational Study from Animal to Human

Measuring occupancy using PET is indispensable in the development of new pharmaceuticals. However, clinical trials for new pharmaceuticals have various restrictions in relation to radiological effects. In-vivo imaging with micro-PET of small animals is a more convenient means, and it is significant for preclinical drug development with the potential of simulating human models.

New concepts of treatment of AD are concerned with directly targeting amyloid in the brain. Vaccination therapy of A β is thought to be a candidate, but how to monitor the treatment is an issue to be settled before entering into any clinical trial. Using amyloid precursor protein (APP) transgenic (Tg) mice, [^{11}C]PIB binding was reduced after vaccination measured by microPET system.[40] Moreover, imaging microglia, which are observed in the vicinity of neuritic plaques, is also important because their activation is responsible for the degree of activity of the brain immune system, and their overactivation causes encephalitis. [^{18}F]FE-DAA1106 is an effective radioligand for peripheral benzodiazepine receptor, and is regarded as an effective biomarker for activated microglia. Using two different ligands for amyloid deposition and microgial activation, a clear relationship between amyloid reduction and the activation of microglia was revealed in vaccinated Tg mice.[44] This result suggests the usefulness of preclinical evaluation of emerging diagnostic and therapeutic approaches for AD.

Saijo and others investigated the occupancies of 5-HTT with rats treated with varying doses of fluvoxamine and a new compound, (2S)-1-[4-(3,4-dichlorophenyl) piperidin-1-yl]-3-[2-(5-methyl-1,3,4-oxadiazol-2-yl) benzo [b] furan-4-yloxy]propan-2-ol monohydrochloride (Wf-516).[45] In that study, a reduction of [^{11}C]DASB binding to 5-HTT was shown to be correlated with the doses and plasma concentrations of fluvoxamine and Wf-516. The estimated ED_{50} value of Wf-516 for [^{11}C]DASB binding was resulted in 3.1 mg/kg (p.o), which was 5 times lower than one of fluvoxamine as 15.2 mg/kg (p.o). This ED_{50} ratio of Wf-516 to fluvoxamine was fairly close to previous ex vivo [3H]citaropram autoradiographic study (Wf-516 vs. fluvoxamine: 1.1 mg/kg vs. 4.5 mg/kg).[46] Moreover, the plasma concentration of fluvoxamine needed for 50% occupancy of central 5-HTT was 6.1ng/ml, similar to the value reported in human studies as 4.6 ng/ml (Fig. 5).[47]

These results suggest preclinical animal PET studies on candidate agents enabling the estimation of the sensitivity and efficacy of pharmacological agents in humans.

However, there are several limitations in current small animal PET studies. The spatial resolution of those PET systems is limited to ~1.5 mm, which is not sufficient for analyzing small brain structures,[48] and the anesthesia used for the fixation of the animal may influence the binding imaging agents.[49,50]

CONCLUSION

In this article, the occupancy by antipsychotics and antidepressants using PET was reviewed. Techniques using PET have made it possible to evaluate how each drug acts at the specific binding site, and provide important indices for evaluating clinical drug efficacy and side effects. Therefore, it is considered that their roles will continue to increase in the psychiatry domain, where there has perhaps been a shortage of objective indices.

REFERENCES

1. Wong DF, Potter WZ, Brasic JR. *Proof of concept: functional models for drug development in humans. In: Davis KL, ed. Neuropsychopharmacology: The Fifth Generation of Progress: Lippincott Williams & Wilkins; 2002. p.457-473.*
2. Seeman P, Lee T. *Antipsychotic drugs: direct correlation between clinical potency and presynaptic action on dopamine neurons. Science 1975;188:1217-1219.*
3. Farde L, Hall H, Ehrin E, Sedvall G. *Quantitative analysis of D_2 dopamine receptor binding in the living human brain by PET. Science 1986;231:258-261.*
4. Farde L, Nordström AL, Wiesel FA, Pauli S, Halldin C, Sedvall G. *Positron emission tomographic analysis of central D_1 and D_2 dopamine receptor occupancy in patients treated with classical neuroleptics and clozapine. Relation to extrapyramidal side effects. Arch Gen Psychiatry 1992; 49:538-544.*
5. Nordström AL, Farde L, Wiesel FA, Forslund K, Pauli S, Halldin C, *et al. Central D_2-dopamine receptor occupancy in relation to antipsychotic drug effects: a double-blind PET study of schizophrenic patients. Biol Psychiatry 1993;33: 227-235.*